Membrane Glycerolipid Remodeling Triggered by Nitrogen and Phosphorus Starvation in *Phaeodactylum tricornutum*[1]

Heni Abida[2], Lina-Juana Dolch[2], Coline Meï[2], Valeria Villanova, Melissa Conte, Maryse A. Block, Giovanni Finazzi, Olivier Bastien, Leïla Tirichine, Chris Bowler, Fabrice Rébeillé, Dimitris Petroutsos*, Juliette Jouhet*, and Eric Maréchal*

Environmental and Evolutionary Genomics Section, Institut de Biologie de l'École Normale Supérieure, Centre National de la Recherche Scientifique Unité Mixte de Recherche 8197, Institut National de la Santé et de la Recherche Médicale, U1024, 75005 Paris, France (H.A., L.T., C.B.); Laboratoire de Physiologie Cellulaire et Végétale, Unité Mixte de Recherche 5168 Centre National de la Recherche Scientifique-Commissariat à l'Energie Atomique-Université Grenoble Alpes, Institut de Recherche en Sciences et Technologies pour le Vivant, Commissariat à l'Energie Atomique Grenoble, 38054 Grenoble cedex 9, France (L.-J.D., C.M., M.C., M.A.B., G.F., O.B., F.R., D.P., J.J., E.M.); and Fermentalg SA, F–33500 Libourne, France (V.V.)

Diatoms constitute a major phylum of phytoplankton biodiversity in ocean water and freshwater ecosystems. They are known to respond to some chemical variations of the environment by the accumulation of triacylglycerol, but the relative changes occurring in membrane glycerolipids have not yet been studied. Our goal was first to define a reference for the glycerolipidome of the marine model diatom *Phaeodactylum tricornutum*, a necessary prerequisite to characterize and dissect the lipid metabolic routes that are orchestrated and regulated to build up each subcellular membrane compartment. By combining multiple analytical techniques, we determined the glycerolipid profile of *P. tricornutum* grown with various levels of nitrogen or phosphorus supplies. In different *P. tricornutum* accessions collected worldwide, a deprivation of either nutrient triggered an accumulation of triacylglycerol, but with different time scales and magnitudes. We investigated in depth the effect of nutrient starvation on the Pt1 strain (Culture Collection of Algae and Protozoa no. 1055/3). Nitrogen deprivation was the more severe stress, triggering thylakoid senescence and growth arrest. By contrast, phosphorus deprivation induced a stepwise adaptive response. The time scale of the glycerolipidome changes and the comparison with large-scale transcriptome studies were consistent with an exhaustion of unknown primary phosphorus-storage molecules (possibly polyphosphate) and a transcriptional control of some genes coding for specific lipid synthesis enzymes. We propose that phospholipids are secondary phosphorus-storage molecules broken down upon phosphorus deprivation, while nonphosphorus lipids are synthesized consistently with a phosphatidylglycerol-to-sulfolipid and a phosphatidycholine-to-betaine lipid replacement followed by a late accumulation of triacylglycerol.

Diatoms are a major component of phytoplankton communities, believed to be responsible for up to one-fourth of global primary productivity (Scala and Bowler, 2001). They live in an environment where light, temperature, pH, oxygen, carbon dioxide, nutrients, and all kinds of physicochemical parameters can vary dramatically. Nitrogen (N), phosphorus (P), and iron are the most often limiting or colimiting nutrients (Mills et al., 2004; Moore et al., 2013), and N is more often limiting than P in marine systems, with the reverse in freshwaters (Hecky and Kilham, 1988). As a selection pressure, the relative fluctuations of N and P have been proposed to be responsible for the differences of size distributions of diatoms, freshwater species being smaller than marine ones due to the ambient scarcity of P (Litchman et al., 2009). Nutrient scarcity is a criterion to define oligotrophic areas in oceans. A study by Van Mooy et al. (2009) on phytoplanktonic communities in an oligotrophic marine region, where P is scarce (less than 10 nM), observed that diatoms reduced their P requirements by synthesizing less phosphoglycerolipids, in particular phosphatidylcholine (PC) and phosphatidylglycerol (PG), and more

[1] This work was supported by the Agence Nationale de la Recherche (grant no. ANR–12–BIME–0005 [DiaDomOil] to C.B., G.F., D.P., and E.M.), the Commissariat à l'Energie Atomique Life Science Division (bioenergy grant EliciTAG to M.C. and E.M.), a European Research Council Advanced Grant (Diatomite; to C.B.), the Centre National de la Recherche Scientifique (Défi Transition Energétique grant to L.T. and G.F.), the OCEANOMICS program from the French Ministry of Research (to E.M.), and the Institut Carnot Lipides pour la Santé et l'Industrie (to E.M.).

[2] These authors contributed equally to the article.

* Address correspondence to dimitris.petroutsos@cea.fr, juliette.jouhet@cea.fr, and eric.marechal@cea.fr.

The author responsible for distribution of materials integral to the findings presented in this article in accordance with the policy described in the Instructions for Authors (www.plantphysiol.org) is: Eric Maréchal (eric.marechal@cea.fr).

H.A., L.-J.D., C.M., V.V., M.C., F.R., D.P., and J.J. performed the experiments; O.B. achieved the bioinformatic analyses; M.A.B., G.F., L.T., and C.B. contributed to the design and analyses of experiments; D.P., J.J., and E.M. designed, supervised, and analyzed the experiments. All authors contributed to the writing of the article.

www.plantphysiol.org/cgi/doi/10.1104/pp.114.252395

nonphosphorus lipids, such as sulfoquinovosyldiacylglycerol (SQDG) and betaine lipids (BL), as compared with communities growing in a P-rich region (more than 100 nM). However, that study did not consider the levels of two other nonphosphorus lipid classes (i.e. the chloroplast galactoglycerolipids, in particular monogalactosyldiacylglycerol [MGDG]) and digalactosyldiacylglycerol (DGDG), and triacylglycerol (TAG). When Van Mooy et al. (2009) examined planktonic membrane lipids at the two locations, their observations were consistent with a PG-to-SQDG and a PC-to-BL replacement triggered by P shortage. In a complementary set of experiments, they cultivated the diatom *Thalassiosira pseudonana* in a P-depleted or P-replete artificial medium and found variations of the SQDG-PG and BL-PC ratios in line with their on-site observations (Van Mooy et al., 2009), supporting that lipid remodeling could be one of the most essential mechanisms allowing a given species to acclimate and populate oligotrophic areas.

Phospholipid-to-nonphosphorus lipid replacement has been studied in depth in the plant Arabidopsis (*Arabidopsis thaliana*; Benning and Ohta, 2005; Shimojima and Ohta, 2011; Boudière et al., 2012; Dubots et al., 2012; Nakamura, 2013; Petroutsos et al., 2014). In Arabidopsis, PC and PG contents decrease upon P starvation, and the synthesis of plastid glycolipids (i.e. MGDG, DGDG, and SQDG) increases coincidentally. Based on the acyl profiles of glycerolipids, it is possible to identify the metabolic routes that are mobilized in this remodeling. In Arabidopsis, MGDG can be synthesized using diacylglycerol (DAG) generated locally inside the plastid, via the so-called prokaryotic pathway, or using diacyl precursors diverted from nonplastid phospholipids, via the so-called eukaryotic pathway (Browse et al., 1986). The prokaryotic structure is characterized by a 16-carbon (C16) fatty acid (FA) at position *sn*-2 of the glycerol backbone, like cyanobacterial lipids, whereas the eukaryotic structure contains an 18-carbon (C18) FA at position *sn*-2. Thus, in Arabidopsis, (1) 18:3/16:3-MGDG originates from the stepwise galactosylation of prokaryotic 18:1/16:0-DAG followed by a rapid desaturation into the trienoic form; and (2) 18:3/18:3-MGDG relies on the import and galactosylation of eukaryotic precursors derived from phospholipids, most notably having 18:2/18:2 structures (Maréchal et al., 1994), also followed by a desaturation into the trienoic form. Upon P shortage, the eukaryotic pathway is activated; PC hydrolysis releases a diacyl intermediate, which is then transferred to the plastid to synthesize MGDG and DGDG (Jouhet et al., 2003), creating a virtuous recycling of lipid intermediates between phospholipid breakdown and galactolipid increase. The Arabidopsis response to low P combines a rapid metabolic regulation, coupling MGDG synthesis to the phospholipid status (Dubots et al., 2010, 2012), with a longer term genomic reprogramming (Misson et al., 2005; Morcuende et al., 2007) characterized by the up-regulation of phospholipases C and D (hydrolyzing phospholipids) and of monogalactosyldiacyl and digalactosyldiacyl isoforms (the galactosyltransferases synthesizing MGDG and DGDG, respectively). In P-starved conditions, a PG-to-SQDG replacement is observed and is considered to be a ubiquitous phenomenon in photosynthetic organisms, enabling the preservation of an anionic lipid environment to the photosystems in the thylakoids (Boudière et al., 2014). No intense trafficking is required for this replacement, as SQDG and PG are both chloroplast lipids. The most spectacular feature of Arabidopsis lipid remodeling consists in the replacement of PC in a variety of subcellular locations, such as the plasma membrane, the tonoplast, and the mitochondria (but not observed in the endoplasmic reticulum [ER]), by DGDG synthesized in the chloroplast, using still uncharacterized lipid export systems (Andersson et al., 2003, 2005; Jouhet et al., 2003, 2004, 2007, 2010; Sandelius et al., 2007; Tjellström et al., 2008).

Lipid modifications triggered in Arabidopsis by a deprivation of N have not been studied as extensively. Upon N shortage, the quantity of N-containing lipids, in particular PC and phosphatidylethanolamine (PE), seems to be unaffected (Gaude et al., 2007). On the other hand, the main response includes a relative decrease of MGDG and an increase of DGDG, concomitant with an up-regulation of the genes encoding both digalactosyldiacyl isoforms, and a small increase of TAG synthesis (Gaude et al., 2007). It is not known whether any lipid trafficking can be triggered by N shortage, nor whether there are any changes in the lipid composition of cell compartments, like those documented in cells exposed to P shortage.

No such comprehensive study has been made in a diatom model. Acyl profiles of all glycerolipid classes and quantifications still have to be determined. The existence of redundant metabolic routes, similar to the prokaryotic and eukaryotic pathways dissected in Arabidopsis, also requires assessment. The conservation of some processes occurring in plants, such as a decrease of MGDG and an increase of DGDG in N-depleted conditions or an increase of MGDG and DGDG and a putative PC-to-DGDG replacement in P-depleted conditions, also should be investigated.

Studies in diatoms have benefited from developments in two model species, the centric diatom *T. pseudonana* (Coscinodiscophyceae) and the pennate diatom *Phaeodactylum tricornutum* (Bacillariophyceae), for which intense efforts have resulted in fully sequenced genomes (Armbrust et al., 2004; Bowler et al., 2008) and provided reference data for transcriptomic (Maheswari et al., 2005, 2009; Allen et al., 2008; Sapriel et al., 2009; Shrestha et al., 2012; Chauton et al., 2013) and whole-cell proteomic (Montsant et al., 2005; Nunn et al., 2009) analyses. *P. tricornutum* is pleiomorphic, with three major morphotypes (fusiform, triradiate, and oval). A series of axenic strains have been collected in various marine environments worldwide, denoted Pt1 to Pt10 (De Martino et al., 2007), allowing analyses of phenotypic variations and the adaptation to various habitats.

In photosynthetic organisms, it is usually considered that, in standard conditions, phospholipids are mostly present in the endomembrane system, whereas nonphosphorus glycolipids are in the plastid. However, this distinction might be more complex in diatoms due to the physical connection between some membranes limiting the plastid with the endomembrane system and/or

mitochondria. Briefly, like all eukaryotes, diatoms contain a conventional endomembrane system comprising the ER, nuclear envelope, Golgi, trans-Golgi network, plasma membrane, etc., which are connected to each other by vesicular shuttles or tubular structures (Brighouse et al., 2010). In addition, two semiautonomous organelles of endosymbiotic origins are present, a mitochondrion limited by two membranes and a plastid bounded by four membranes, which originate from a secondary endosymbiosis (Dorrell and Smith, 2011; Petroutsos et al., 2014). A continuum occurs between the ER and the outermost membrane of the plastid (Kroth et al., 2008). The glycerolipid composition of each of the four membranes that surround the plastid is simply unknown. Therefore, it is difficult to speculate on the location of MGDG and DGDG synthesis and whether any export of DGDG to other locations of the cell could be plausible, like that observed in plants. Given the current state of membrane fractionation techniques, only global analyses can be performed. By contrast with other omics data, and although previous targeted studies have allowed the structural determination of some isolated glycerolipid classes (Arao et al., 1987; Yongmanitchai and Ward, 1993; Naumann et al., 2011), the complete membrane glycerolipidome of *P. tricornutum* has not been fully characterized. The analyses of membrane glycerolipid remodeling in diatoms should also consider the accumulation of TAG triggered by nutrient shortage, which has been scrutinized in much more detail due to the potential applications for biofuels and green chemistry (Alonso et al., 2000; Rezanka et al., 2011; Zendejas et al., 2012; Levitan et al., 2014).

In this article, by combining multiple analytical techniques, we sought to characterize comprehensively the major membrane glycerolipid classes in *P. tricornutum*, together with TAG. FA profiles of each class have been determined, providing acyl signatures that can be used as markers for diacyl moiety origins and fluxes. With a fully characterized glycerolipidome in hand, we then analyzed changes triggered by N and/or P depletion and deduced from lipid class and acyl signature variations the dynamic processes driving the observed lipid remodeling.

RESULTS

Comparison of *P. tricornutum* Ecotypes in Nutrient-Replete and Nutrient-Limiting Batch Cultivation

We examined the responses of all available *P. tricornutum* accessions, collected originally in various geographical regions and covering all known morphotypes (i.e. the fusiform shape commonly observed in laboratory conditions, the triradiate shape thought to be more abundant in nature, and the oval shape, indicative of a temperature or salinity stress; De Martino et al., 2007; Fig. 1A). In our growth conditions, most accessions were fusiform except Pt8, which is mainly triradiate, and Pt3 and Pt9, which are oval. Cells grown in nutrient-replete conditions (0.55 mM N and 0.0224 mM P, called here 1N1P) were shifted to −N (0N1P) or −P (1N0P) medium.

Nonpolar lipid accumulation (mainly TAG), known to be triggered by nutrient shortage in phytoplankton, was monitored using Nile Red fluorescence staining. N depletion triggered a faster TAG accumulation as compared with P depletion; therefore, the comparison of the response of the different ecotypes to −N or −P was made 3 d after N depletion (Fig. 1B) and 8 d after P depletion (Fig. 1C). All accessions showed a marked accumulation of TAG shortly after N depletion, except Pt4, which exhibited a relatively modest increase (a representative experiment is shown in Figure 1B). The detection of nonpolar lipid accumulation in response to low P required a much longer cultivation time in P-depleted medium, and no significant TAG accumulation could be detected after 3 to 5 d. After 8 d of growth in a P-limited medium, a contrasting phenotype in the series of Pt accessions could be observed (a representative experiment is shown in Figure 1C), with a substantial accumulation of nonpolar lipid in all accessions except Pt4, Pt10, and PtHK, in which the Nile Red staining was lower than a 2-fold increase, as compared with cells grown in a replete medium.

We did not observe any correlation between the magnitude of response to N or P depletion and the corresponding morphotypes. Phenotypic variations might be related, rather, to the efficiency of N or P storage systems in the different accessions and/or to the signaling and metabolic processes activated by the lack of nutrients. In all cases, an increase of Nile Red fluorescence, even moderate, was always detected, thus demonstrating that TAG accumulation is a marker of nutrient shortage. We decided to pursue our experiments on Pt1, the most commonly used strain in laboratories, which responded significantly to both N and P deprivations.

Effects of N and P Depletion on the Growth and Photosynthesis of *P. tricornutum*

Since P depletion exerted an effect after a longer time period than N depletion, we had to be sure, when studying the effect of P shortage, that no exhaustion of N occurred during the time of observation and that control conditions were indeed kept replete. To avoid such issues, we adjusted the initial nutrient-replete conditions to concentrations 10 times higher than that applied in our comparative study of ecotypes (i.e. 5.5 mM N and 0.22 mM P [a medium called 10N10P]). We checked that the 10N10P medium supported the growth of *P. tricornutum* Pt1 at higher cell densities compared with the 1N1P medium (Supplemental Fig. S1A). Most importantly, the photosynthetic capacity of cells, probed as photosynthetic capacity (F_v/F_m), remained unaltered for 10 d in the 10N10P medium, in stark contrast with cells grown in 1N1P medium, where F_v/F_m dropped quickly during the growth period (Supplemental Fig. S1B). After 5 d of cultivation in 1N1P medium, a decrease of F_v/F_m and an increase of nonpolar lipid content were measured

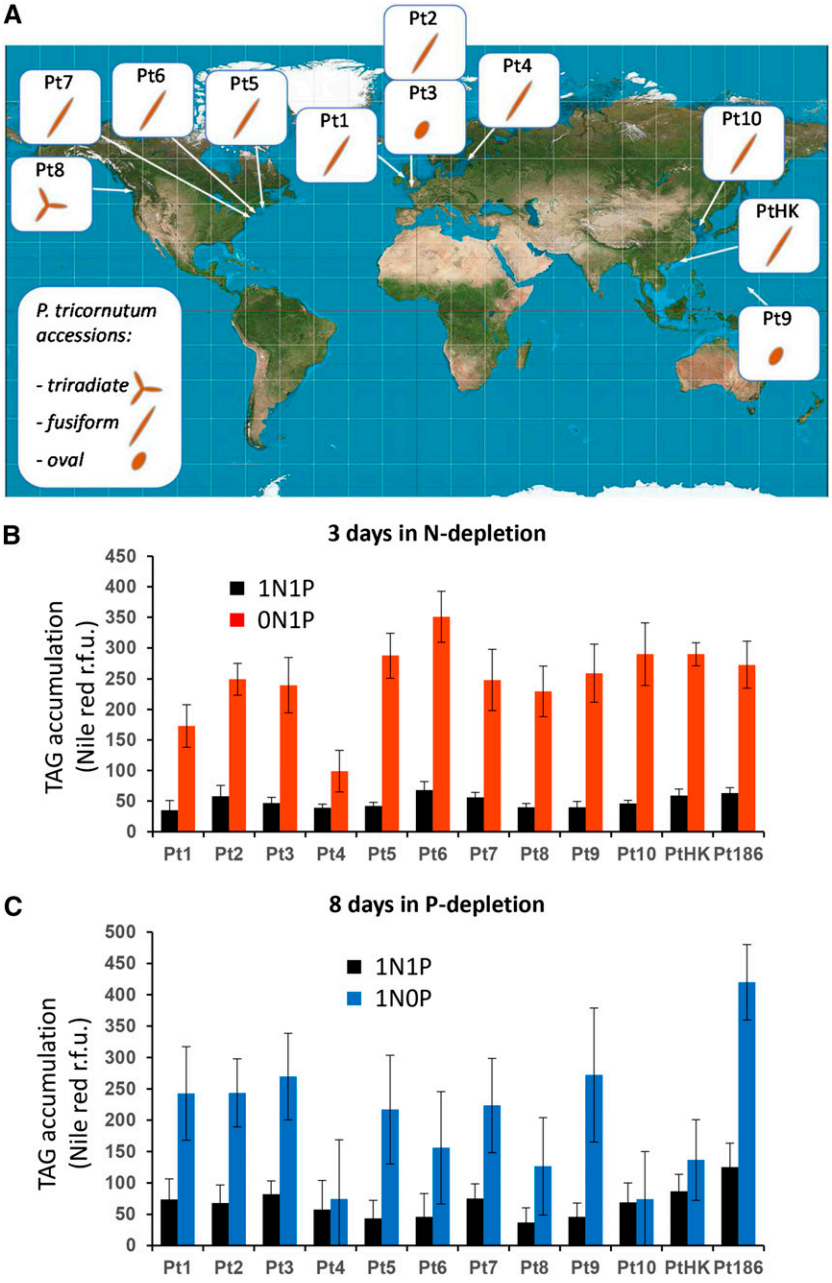

Figure 1. Preliminary comparison of accessions of *P. tricornutum* grown in artificial medium depleted in N or P. A, Geographical origin and major morphotypes of Pt accessions. The origin areas of sampling of Pt accessions are shown: Pt1 off Blackpool, United Kingdom; Pt2 and Pt3 off Plymouth, United Kingdom; Pt4 near the island of Segelskå; Pt5 in the Gulf of Maine; Pt6 off Woods Hole, Massachusetts; Pt7 off Long Island, New York; Pt8 near Vancouver, Canada; Pt9, Territory of Guam, Micronesia; PtHK, near Hong Kong; and Pt10, in the Yellow Sea. The genomic strain Pt1 8.6 derives from the Pt1 accession. Pt3 is a stress form deriving from Pt2. Major morphotypes observed for each accession in artificial seawater are indicated (i.e. the triradiate, fusiform, and oval morphotypes; from De Martino et al. [2007]). B, Accumulation of nonpolar lipids in N-limiting conditions. Cells in the exponential phase of growth were harvested by centrifugation and transferred to a fresh replete (1N1P; black bars) or N-depleted (0N1P; red bars) ESAW medium. Nonpolar lipid accumulation was measured after 3 d by Nile Red staining and expressed as fluorescence intensity normalized by cell number. C, Accumulation of nonpolar lipids in P-limiting conditions. Cells in the exponential phase of growth were harvested by centrifugation and transferred to a fresh replete (1N1P; black bars) or P-depleted (1N0P; blue bars) ESAW medium. Nonpolar lipid accumulation was measured after 8 d by Nile Red staining and expressed as fluorescence intensity normalized by cell number. r.f.u., Relative fluorescence units.

(Supplemental Fig. S1C), reflecting a nutrient limitation in the 1N1P medium that did not occur in the 10N10P condition.

We then evaluated the time scale of the Pt1 response after transfer to nutrient-limiting conditions. For this, the diatoms were grown in 10N10P medium until they reached a cell density of 6 to 7 million cells mL^{-1}. Cells were centrifuged, washed with 0N0P medium, and resuspended in 10N10P, 0N10P, and 10N0P media at a starting cell density of 3 to 3.5 million cells mL^{-1}. N depletion resulted in growth arrest after 1 d (Supplemental Fig. S2A) and led to an accumulation of nonpolar lipids after 4 d (based on Nile Red fluorescence; Supplemental Fig. S2B). P depletion affected neither growth nor lipid accumulation between days 0 and 4 (Supplemental Fig. S2, A and B), consistent with the delay observed for the different accessions grown in 0N1P or 1N0P medium, before any visible effect could be measured (Fig. 1, B and C).

We then cultivated Pt1 cells in sufficient amounts to analyze in parallel their cell phenotypes, photosynthetic properties, and lipidomic profiles. Based on previous experiments (Supplemental Fig. S2B), F_v/F_m was selected as an indicator of nutrient limitation (Fig. 2A). At day 5, cells grown in 10N10P and 0N10P were harvested, whereas cells grown in 10N0P were kept in the culture medium until day 13. We should note that at days 5, 8, and 10, 30% of the 10N0P culture volume was replaced by fresh 10N0P medium to ensure that no other

nutrient limitation besides P would occur. In parallel, a 10N10P culture was similarly complemented with fresh 10N10P medium and kept as a control condition during the same period. After 13 d of P limitation, the cells were clearly impacted in their photosynthetic activity (Fig. 2A) and showed a high nonpolar lipid content (Fig. 2B). At the same time point, the control cultures also showed a slightly diminished F_v/F_m, which was not attributed to N or P deprivation, since we did not observe any TAG accumulation (Fig. 2B). Since we did not detect any significant change in the TAG content and membrane glycerolipid profile of cells grown in 10N10P medium collected after 5 or 13 d of culture, we used cells collected after 5 d in 10N10P as a control to compare nutrient-starved and nutrient-replete cells.

Comprehensive Characterization of the Glycerolipid Content of *P. tricornutum* Pt1 Grown in Nutrient-Replete Medium

We extracted the lipids from *P. tricornutum* cells with great caution to avoid lipid degradation. For this purpose, samples were freeze dried rapidly after harvest and lipids were extracted following a treatment in boiling ethanol to inactivate lipase activities. An aliquot fraction of the total extract of glycerolipids was transesterified in the presence of methanol, thus producing fatty acid methyl esters (FAMEs) that were separated by gas chromatography and quantified by flame ionization detection (GC-FID), as described in "Materials and Methods." We used thin-layer chromatography (TLC) to separate the different classes of glycerolipids, combining robust one-dimensional and two dimensional TLC systems to separate, on the one hand, nonpolar glycerolipids and free FA, and on the other hand, polar glycerolipids (phosphoglycerolipids and nonphosphorus glycerolipids; Fig. 3; Supplemental Fig. S3). We analyzed the structure of lipids in each spot revealed on the TLC plate (see "Materials and Methods") by mass spectrometry (MS; Tables I–III) and determined the corresponding FAME profiles by GC-FID.

The total glycerolipid extract from *P. tricornutum* grown in a 10N10P medium had a FA composition similar to those already reported in the literature for diatoms (Guschina and Harwood, 2006; Liang et al., 2014) and eustigmatophytes such as *Nannochloropsis graditana* (Simionato et al., 2013): that is, strikingly enriched in C16 molecular species (16:0, 16:1, 16:2, and 16:3) and eicosapentaenoic acid (20:5) and poor in C18 FAs (Fig. 4A).

We analyzed the different classes of glycerolipids in the extract (Fig. 4B), providing, to our knowledge, the first reference for a complete glycerolipidome of *P. tricornutum* in unstressed conditions. The profile is dominated by MGDG, SQDG, and PC, which together represent more than 75% of the total content. We also confirmed the presence of 20:5 acyl-SQDG, as reported previously (Naumann et al., 2011; Supplemental Fig. S4). We identified a spot corresponding to diacylglyceryl-hydroxymethyl-*N*,*N*,*N*-trimethyl-β-alanine (DGTA; Figs. 3 and 4B; Supplemental Fig. S3), a betaine glycerolipid that had not yet been reported for *P. tricornutum* but has been reported for other algae such as *Phaeocystis* sp. (Haptophycea), *Ochromonas danica* (Chrysophyceae),

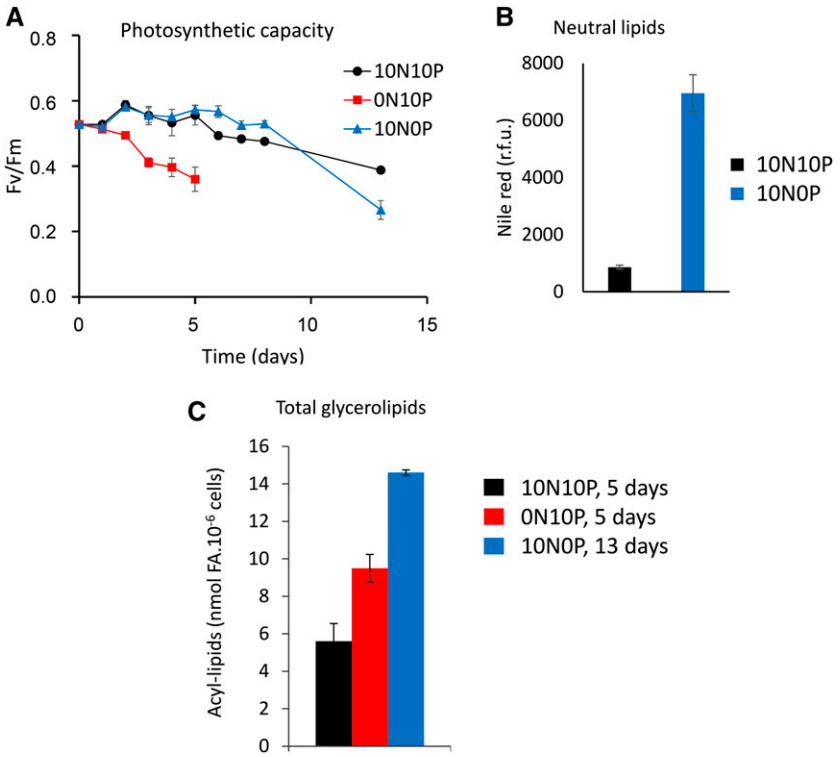

Figure 2. Photosynthetic activity and lipid accumulation in the Pt1 ecotype of *P. tricornutum* cultivated in replete or N- or P-depleted conditions. A, Time-course evolution of photosynthetic efficiency. The F_v/F_m ratio, representative of the photosynthetic efficiency of the diatom, was measured for Pt1 cells grown either in a replete medium (10N10P; black) or in medium deprived of N (0N10P; blue) or P (10N0P; red). B, Nonpolar lipid accumulation measured at day 13. Nonpolar lipid accumulation was estimated by Nile Red fluorescence normalized to cell number. In 10N10P, the fluorescence signal remained at background level, indicating that the F_v/F_m decrease was not due to N or P starvation. r.f.u., Relative fluorescence units. C, Total glycerolipid accumulation. The total level of glycerolipids (membrane lipids + TAG) was estimated by the total FA content after 5 d of cultivation in the replete condition (black bar) or following N starvation (red bar) or 13 d of P starvation (blue bar). To avoid any N deficiency in 10N10P or 10N0P culture, the media were replaced by fresh ESAW 10N10P medium every 3 d.

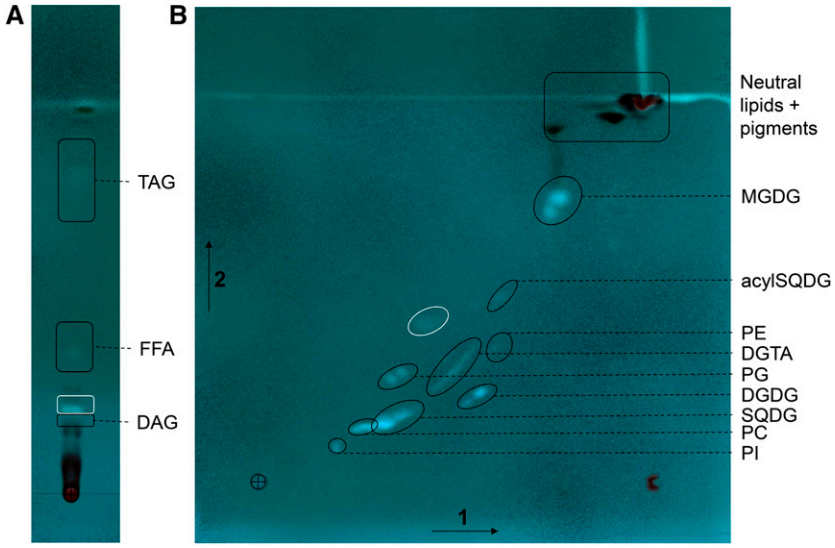

Figure 3. Separation by TLC of the glycerolipids from *P. tricornutum*. Lipids from Pt1 cells grown in a replete medium (10N10P) were extracted and resolved following the procedures described in "Materials and Methods." The cross indicates the initial deposit. A, One-dimensional separation of nonpolar lipids (DAG and TAG) and free FA (FFA). Migration was performed in hexane:diethylether:acetic acid (70:30:1, v/v). B, Two-dimensional separation of polar (membrane) lipids. Migration was performed in chloroform:methanol:water (65:25:4, v/v) for the first dimension (arrow 1) and chloroform:acetone:methanol:acetic acid:water (50:20:10:10:5, v/v) for the second migration (arrow 2). Lipids were visualized under UV light, after spraying with 2% 8-anilino-1-naphthalenesulfonic acid in methanol, and scraped off the plate for analyses. Identification of the lipid in each spot was performed by MS2 analyses. The spot circled in white is an unknown compound with a structure that differs from a glycerolipid.

and some brown algae such as *Fucus vesiculus* (Phaeophyceae; Dembitsky, 1996). DGTA has the same mass as diacylglyceryl-*N*,*N*,*N*-trimethylhomoserine (DGTS) but could be discriminated by a different migration position on two-dimensional TLC (Vogel and Eichenberger, 1992) and, following tandem mass spectrometry (MS2) fragmentation, by the absence of a fragment corresponding to a loss of mass-to-charge ratio (*m/z* 87; Armada et al., 2013). We did not detect the presence of DGTS in *P. tricornutum*.

Nonpolar lipids, DAG and TAG, are also present but in minor amounts (e.g. TAG represented only 1%–3% of the total glycerolipids when cells were grown in the 10N10P medium; Fig. 4B). We were not able to identify in our TLC system any spot corresponding to phosphatidic acid, diphosphatidylglycerol, and phosphatidyl-Ser. This does not mean that these phospholipids are absent in *P. tricornutum* but indicates that they each represent less than 1% of the total glycerolipid content. Overall, the main lipids are the four chloroplast lipids present in every photosynthetic membrane (i.e. MGDG, SQDG, DGDG, and PG) together with PC, which is usually the main glycerolipid in nonplastid membranes, although in diatoms its abundance in the four membranes surrounding the chloroplast cannot be excluded.

The positioning of FAs on each glycerolipid (summarized in Table III) was determined using MS and MS2 analyses, as described in Table II. The FA molar profiles (percentage) of the three main membrane lipids and the nonpolar glycerolipids are shown in Figure 5.

Several general features can be deduced from Table III. First, we confirmed previous analyses (Arao et al., 1987; Yongmanitchai and Ward, 1993) reporting that 16:3 is always located at the *sn*-2 position and 20:5 at the *sn*-1 position, except when two 20:5s are present. Almost all glycoglycerolipids have a C16 FA at the *sn*-2 position, suggesting that the plastid lysophosphatidic acid acyltransferase (LPAAT), an enzyme called Arabidopsis seed gene2 (ATS2) in plants, has a very high selectivity for a C16-acyl carrier protein (C16-ACP), as in higher plants (Frentzen et al., 1983), and that the plastid pathway (also known as the prokaryotic pathway) for the synthesis of the diacylglycerol backbone of glycoglycerolipids is largely dominant in diatoms (Mongrand et al., 1998). Considering MGDG, for example, the most abundant species is 20:5/16:3, in agreement with our gas chromatography analyses (Fig. 5). Generally speaking, 16:3 and 16:4 are restricted to MGDG and only found at the *sn*-2 position. Considering DGDG, synthesized from MGDG, the *sn*-2 position is also esterified exclusively to a C16-FA, suggesting that these molecular species could originate from the same plastidic pathway. FAs in the *sn*-2 position are more saturated than those in MGDG (no 16:3 and 16:4 could be detected), suggesting that the desaturation of MGDG in 16:3 and 16:4 could be a way to lock an MGDG diacylglycerol backbone, preventing its utilization as a substrate for the synthesis of other glycerolipids, as shown previously in plants (Boudière et al., 2012; Petroutsos et al., 2014) and in *Chlamydomonas reinhardtii* (Li et al., 2012). By contrast with plants, the *sn*-1 position of MGDG contains a very low proportion of C18 molecular species, with only about 8% of 18:0/16:3. The acyl profile of the different lipid classes, therefore,

Table I. *Identification of glycerolipids from P. tricornutum*

Characteristic fragments generated by fragmentation of the parent ion (MS2) are shown, together with the associated references.

Analyzed Lipids	Polarity	Ion Analyzed	Specific Fragments in MS2 Scan	References
Phospholipids				
PC	+	$[M + H]^+$	Neutral loss of *m/z* 59	Domingues et al. (1998)
PE	+	$[M + H]^+$	Neutral loss of 141	Brügger et al. (1997)
Phosphatidylserine	+	$[M + H]^+$	Neutral loss of 185	Brügger et al. (1997)
PG	+	$[M + NH_4]^+$	Neutral loss of 189	Taguchi et al. (2005)
PI	+	$[M - H]^-$	Precursors of *m/z* 241	Hsu and Turk (2000b)
Phosphatidic acid	+	$[M + NH_4]^+$	Neutral loss of 115	Li-Beisson et al. (2010)
Nonphosphorus glycerolipids				
SQDG	–	$[M - H]^-$	Precursors of *m/z* 225	Gage et al. (1992); Welti et al. (2003)
ASQ	–	$[M - H]^-$	Precursors of *m/z* 509	Naumann et al. (2011)
MGDG	+	$[M + NH_4]^+$	Neutral loss of 179	Li-Beisson et al. (2010)
DGDG	+	$[M + NH_4]^+$	Neutral loss of 341	Moreau et al. (2008)
DGTA	+	$[M + H]^+$	Precursors of *m/z* 236; neutral loss of 59; no neutral loss of 87 as found for DGTS	Armada et al. (2013)
Neutral glycerolipids				
Free FA	–	$[M - H]^-$		
DAG	+	$[M + NH_4]^+$	Scan of $[M+NH_4\text{-}RCOONH_4]^+$	Camera et al. (2010)
TAG	+	$[M + NH_4]^+$	Scan of $[M+NH_4\text{-}RCOONH_4]^+$	Hsu and Turk (2010)

indicates (1) that the FA synthases of the chloroplast produce 14:0, 16:0, and 18:0 species, (2) that the acyl-ACP Δ9-desaturase is mainly active on 16:0 rather than on 18:0, and (3) that the plastid glycerol-3-phosphate acyltransferase (an enzyme called ATS1 in plants) may have a lower affinity for C18 substrates than plant ATS1. The relative availability of acyl-ACP substrates (C16, C18, and C20 molecular species) also might be an important determinant, as it was recently reported that the level of C18 FA increased in MGDG when shifting the growth temperature from 20°C to 30°C, a condition known to lower 20:5 biosynthesis (Dodson et al., 2014).

PE, PC, and DGTA, which are likely synthesized in extraplastidic membranes, also contain C16 species at the *sn*-2 position, together with C18 and C20 FAs. The occurrence of a C16 FA at the *sn*-2 position in this lipid is consistent with two hypotheses: either an export of a prokaryotic diacylglycerol backbone or the fact that the microsomal LPAAT has no selectivity for FA molecular species, by contrast with the plastid LPAAT. Thus, in *P. tricornutum*, no specific signature could be determined for a potential eukaryotic pathway providing diacyl precursors to plastid lipids, as defined, respectively, in Arabidopsis and other microalgae such as *C. reinhardtii* (Fan et al., 2011). A similar unbiased chain-length incorporation at the *sn*-2 position in *P. tricornutum* has also been observed in some chlorophytes such as *Dunaliella bardawil* (Davidi et al., 2014), despite their distant lineages. In addition, PE, PC, and DGTA retained most of the C18 present in the cells. It is also noteworthy that we

Table II. *Conditions for the regiochemical assignment of FAs at sn-1, sn-2, and sn-3 positions in glycerolipids from P. tricornutum*

Analyzed Lipids	Polarity	Ion Analyzed	MS2 Fragment Properties	References
Phospholipids				
PC	+	$[M + H]^+$	$[M+H\text{-}R_2CH = C = O]^+ > [M+H\text{-}R_1CH = C = O]^+$	Hsu and Turk (2003)
PE	–	$[M - H]^-$	$[R_2COO]^- > [R_1COO]^-$	Hsu and Turk (2000a)
PG	–	$[M - H]^-$	$[M\text{-}H\text{-}R_2COOH]^- > [M\text{-}H\text{-}R_1COOH]^-$	Hsu and Turk (2001)
PI	–	$[M - H]^-$	$M\text{-}H\text{-}R_2COOH]^- > [M\text{-}H\text{-}R_1COOH]^-$	Hsu and Turk (2000b)
Nonphosphorus glycerolipids				
SQDG	–	$[M - H]^-$	$[M\text{-}H\text{-}R_1COOH]^- > [M\text{-}H\text{-}R_2COOH]^-$	Zianni et al. (2013)
ASQ	–	$[M - H]^-$	$[M\text{-}H\text{-}R_1COOH]^- > [M\text{-}H\text{-}R_2COOH]^-$	Naumann et al. (2011)
MGDG	+	$[M + Na]^+$	$[M+Na\text{-}R_1COO^-]^+ > [M+Na\text{-}R_2COO^-]^+$	Guella et al. (2003)
DGDG	+	$[M + Na]^+$	$[M+Na\text{-}R_1COO^-]^+ > [M+Na\text{-}R_2COO^-]^+$	Guella et al. (2003))
DGTA	+	$[M + H]^+$	$[M+H\text{-}R_2COOH]^+ > [M+H\text{-}R_1COOH]^+$	By analogy with phospholipid diacylglycerol moiety
Nonpolar glycerolipids				
DAG	+	$[M + NH_4]^+$	$[M+NH_4\text{-}R_1COONH_4]^+ > [M+NH_4\text{-}R_1COONH_4]^+$	Camera et al. (2010)
TAG	+	$[M + NH_4]^+$	$[M+NH_4\text{-}R_{1/3}COO^-]^+ > [M+ NH_4\text{-}R_2COO^-]^+$	Hsu and Turk (2010)

Table III. *Positional distribution of FAs, and molecular species found in each glycerolipid class*

Only molecules that represent more than 5% of all the species present in the class are indicated. The asterisk indicates where the *sn*-1 and *sn*-2 positions could not be discriminated. Major molecular species of a given lipid class are shown in bold characters.

sn-1/*sn*-2	MGDG	DGDG	SQDG	ASQ	PG	PC	DGTA	PE	PI	DAG	TAG
14:0/16:0			6.9	6							
14:0/16:1			16.5	13.2						14.5	
16:0/16:0			4.6								
16:1/16:0	5.2	8.7	**23.9**	8.2	**31.7**				**100**	**54.8***	
16:1/16:1	6.6	14.1			4.9	5.2	5.1			**30.8**	
16:1/16:2		5.4									
16:1/16:3	7.9										
16:1/18:1	5.4										
16:1/24:0			9.7								
16:2/16:0			9.6								
16:2/16:3	10.5										
18:0/16:3	7.7										
18:2/18:2						5.2					
20:5/14:0				12.7							
20:5/16:0		6.6	9.4	**53.5**	11.2	6.9					
20:5/16:1		16.1			**48.5**	12.1	**13**	11.3			
20:5/16:2	5.1	**34.3**				5	5.2	6.4			
20:5/16:3	**19.1**	7.3									
20:5/16:4	7.4										
20:5/18:2							7	7.8			
20:5/18:3						7	4.9	5.6			
20:5/18:4							5.7	6.2			
20:5/20:4						7.2		9.2			
20:5/20:5						**20.1**	**11.1**	**24**			
sn-1/*sn*-2/*sn*-3											
14:0/16:1/16:1											6.5
14:0/16:1/16:0											9.3
16:1/16:1/16:1											11
16:1/16:1/16:0											**23.5**
16:1/16:0/16:0											**16**
16:1/16:0/20:5											5

found only one species of phosphatidylinositide (PI), with a 16:1/16:0 scaffold, suggesting a peculiar role for this phospholipid. PG showed two major species, 20:5/16:1 and 16:1/16:0, always with a C16 at position *sn*-2. It was reported previously that 16:1 at the *sn*-1 position was 16:1 (*ω*-7) (cis-desaturation in *ω*-7 or Δ-9 position) and 16:1 at the *sn*-2 position was 16:1(*ω*-13)t (trans-desaturation at position *ω*-13; Arao et al., 1987). Because the C16 trans-isomer is found only in chloroplast PG, it is likely that the 20:5/16:1 PG is located in plastids and that the 16:1/16:0 PG, similar to PI, is an extraplastidic PG species.

We also found that acyl-SQDG always harbors a 20:5 linked to its polar head, with the same diacylglycerol backbones as those found in SQDG species but with a highly dissimilar distribution. The main species of 20:5 acyl-SQDG was 20:5/16:0, and the corresponding SQDG substrate represented only 10% of its own class of lipid. Assuming that acylation occurs on SQDG (Riekhof et al., 2003), this observation suggests that it should be quite specific for the molecular species 20:5/16:0.

Concerning nonpolar lipids, the DAG pool is mainly constituted of three different molecular species, dominated by 16:1/16:0 and 16:1/16:1, with a lower amount of 14:0/16:1. Although minor amounts of C18 and C20 were detected in DAG by gas chromatography analysis (Fig. 5), these FAs were not detected by MS analyses, indicating that DAG species having a C18 or C20 were minor and could not be discriminated from the background. The DAG acyl composition (Table III) does not reflect the composition found in the main membrane lipids, in support of a de novo synthesis rather than a recycling of the diacylglycerol backbone from membrane lipids. These DAG molecular species are clearly at the origin of the TAG pool, also dominated by 16:0 and 16:1, with lower amounts of 14:0 and some 20:5 at position *sn*-3 (or *sn*-1). The proportion of TAG among other glycerolipids was low, reflecting the absence of any nutrient limitation.

Based on our structural determination of glycerolipid classes, we thus generated a reference profile for glycerolipids in *P. tricornutum* grown in nutrient-replete conditions. Based on this, we then assessed the variation of the glycerolipidome in nutrient-limited cells.

Impact of N and P Shortage on the Glycerolipid Content of *P. tricornutum* Pt1

We analyzed the glycerolipid profile in *P. tricornutum* Pt1 cells after 5 d of N starvation and 13 d of P starvation:

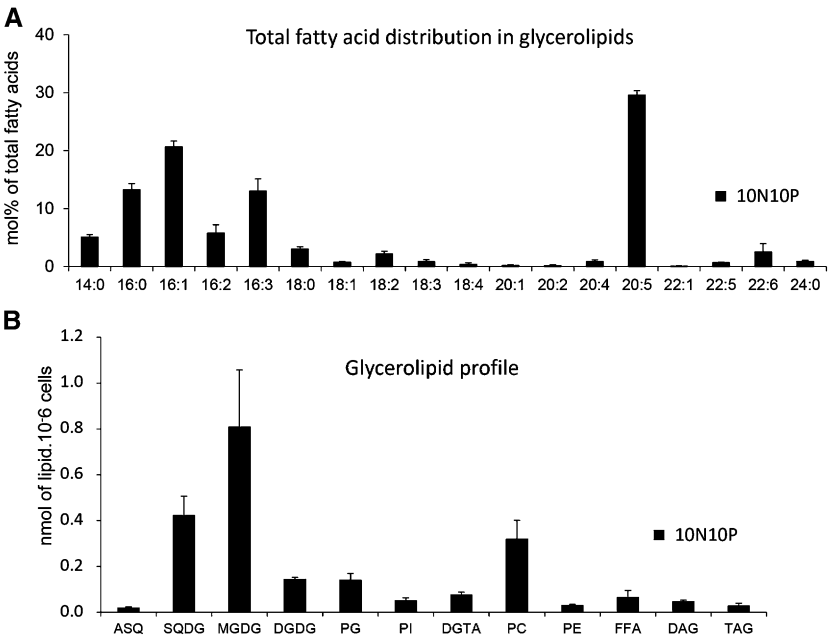

Figure 4. Quantitative analysis of *P. tricornutum* glycerolipids. Lipids from Pt1 cells grown in a replete medium (10N10P) were extracted, separated by TLC, and analyzed as described in "Materials and Methods." A, Global FA profile in a total lipid extract. FA proportions are given in percentages. B, Quantitative analysis of the various glycerolipids identified after TLC separation. Glycerolipids are expressed in nmol 10^{-6} cells and not as the summed FA content in each class. Each result is the average of three biological replicates ± SD. ASQ, 20:5-Acyl-SQDG; FFA, free FAs.

that is, when strong impacts on both the photosynthetic capacity (based on the F_v/F_m ratio) and the nonpolar lipid content (based on Nile Red staining) could be observed (Figs. 1 and 2). Figure 6A shows the glycerolipid profile in the three contexts: control (10N10P), N oligotrophic (0N10P), and P oligotrophic (10N0P). We observed the following trends. (1) A considerable increase of TAG content, on a per cell basis, was observed in both N- and P-limiting conditions, reaching 40 and 60%, respectively, of the total glycerolipid content (i.e. a 45-fold and a 100-fold increase when compared with control conditions). (2) The MGDG content decreased in both conditions. This decrease was more pronounced in the case of N shortage, whereas the levels of the other membrane lipids remained almost unchanged, except for PG, which also decreased by a factor of 2. (3) A total disappearance of the phospholipids was observed in the P-starved condition, including the major phospholipids PC and PG, coinciding with a strong increase of DGTA and slight increases of DGDG and SQDG.

The nature and amounts of FA, measured as a whole (Fig. 6B), were also affected by nutrient limitation, with marked increases of 16:0 and 16:1 and a smaller albeit significant increase of 14:0, in support of an induced FA neosynthesis. Interestingly, the total amount of 20:5, the dominant FA in the control condition, remained almost unchanged. Thus, in the nutrient-limiting conditions, the dominant FA is no longer 20:5 but 16:1. Generally speaking, with the notable exception of TAG, the FA composition remained unchanged in the different glycerolipids (data not shown). A specific focus on TAG (Fig. 6C) indicated that not only 14:0, 16:0, and 16:1 but also 20:5 increased. In fact, the proportion of 20:5 in this class of lipids increased from about 1% in the control conditions to 8% in the N-starved and 6% in the P-starved conditions, suggesting a specific enrichment of 20:5 in TAG. MS analysis indicated that 20:5, as observed in control cells, was esterified at the *sn*-3 (or *sn*-1) position, indicating that this FA had been incorporated during the latter phases of TAG biosynthesis.

In order to better understand the origin of these FAs accumulating in TAGs, we measured the amount of 16:1 and 20:5 in each glycerolipid (Fig. 7A). The level of 16:1 remained approximately constant in all glycerolipids except in TAG, indicating that the observed increase of 16:1 (Fig. 6B) was mainly, if not only, correlated to the increase of TAG synthesis and reflected FA neosynthesis. In the N-starved condition, the level of 20:5 increased in TAG and decreased in MGDG by about the same amount (Fig. 7B). Because it almost remained constant in the other glycerolipids, this result suggests a 20:5 transfer from MGDG to TAG, as observed previously in *N. graditana* (Simionato et al., 2013) and *C. reinhardtii* (Fan et al., 2011).

In the P-limiting conditions, the situation was more complex. A stronger increase of 20:5 was observed in the TAG pool, together with a smaller decrease in the MGDG pool than was observed in N-starved cells. No phospholipid, containing initially a high proportion of 20:5, could be detected. Recycling of phospholipid FAs, therefore, also could contribute to the 20:5 enrichment of TAG. Furthermore, an increase of SQDG and DGTA was observed (Fig. 6A), consistent with (1) a PG replacement by SQDG in the plastid and (2) a possible recycling of the PC diacylglycerol moiety into DGTA, taking place in an extraplastidic membrane. This hypothesis is based on the strong increase of 20:5 in DGTA, likely reflecting the quantitative increase of the DGTA pool (Fig. 6A) rather than a specific 20:5 enrichment, because the global FA composition remained largely unaffected.

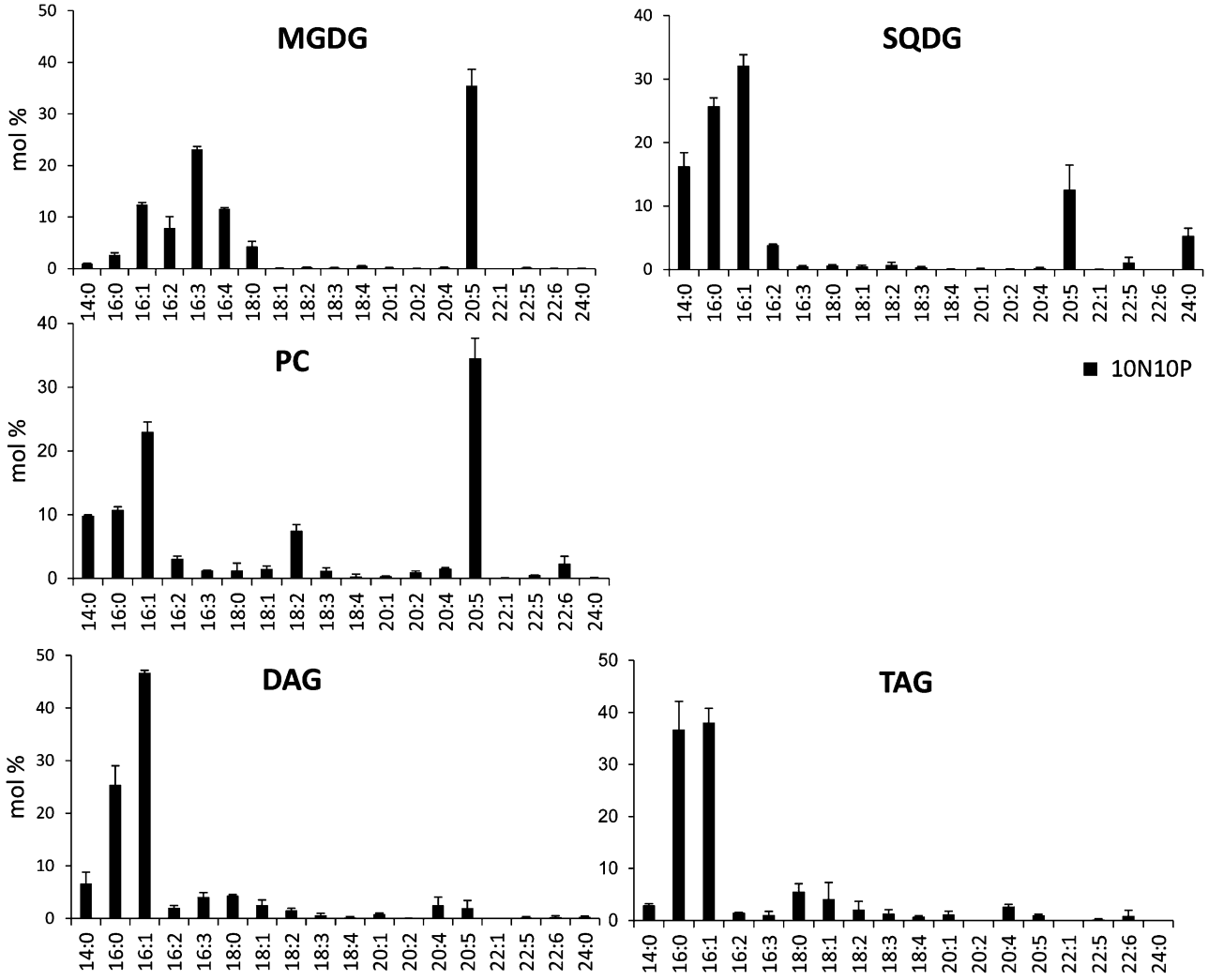

Figure 5. Molar profiles of FAs in PC, DAG, TAG, MGDG, and SQDG. Lipids from Pt1 cells grown in a replete medium (10N10P) were extracted, separated by TLC, and analyzed for their FAs as described in "Materials and Methods." Note that a cross contamination is possible between SQDG and PC due to the proximity of the TLC spots, leading to moderate enrichment of 20:5 in SQDG and 14:0 in PC. Each result is the average of three biological replicates ± SD.

DISCUSSION

A Reference Glycerolipid Profile for *P. tricornutum*

The glycerolipid composition of *P. tricornutum* presents a strong similarity with those reported for other photosynthetic unicellular eukaryotes (Dembitsky, 1996) but also specific differences. Besides the major lipids conserved in photosynthetic membranes (i.e. MGDG, DGDG, SQDG, and PG), we confirmed the presence of 2′-*O*-acylsulfoquinovosyldiacylglycerides (20:5-acyl-SQDG [ASQ]), largely dominated by the molecular species *sn*-1:20:5/*sn*-2:16:0/2′:20:5 (Naumann et al., 2011). The presence of ASQ has also been reported for *C. reinhardtii*, although 18:3 or 18:4 acyl groups were the FAs involved in the 2′-acylation of the sulfoquinovose moiety (Riekhof et al., 2003). To date, there is no evidence for a physiological or biochemical role of ASQ. The large proportion of SQDG also suggests that this lipid might not be restricted to chloroplast membranes; therefore, the subcellular localization of SQDG and ASQ should be assessed in the future.

Notwithstanding, an *SQD1 C. reinhardtii* mutant, lacking SQDG and ASQ, was clearly impaired in its photosynthetic capacities and in its response to inorganic phosphate deficiency, indicating altered membrane properties and an inability to adjust its membrane composition to adapt to environmental change (Riekhof et al., 2003). These experiments did not reveal any specific role of ASQ versus SQDG, but the results presented here indicate that, if SQDG is the precursor of ASQ, as postulated previously (Riekhof et al., 2003), this acylation process is quite specific for one minor SQDG species, *sn*-1:20:5/*sn*-2:16:0, representing less than 10% of the total SQDG. Such specificity in the acylation process suggests the existence of a specific role for ASQ.

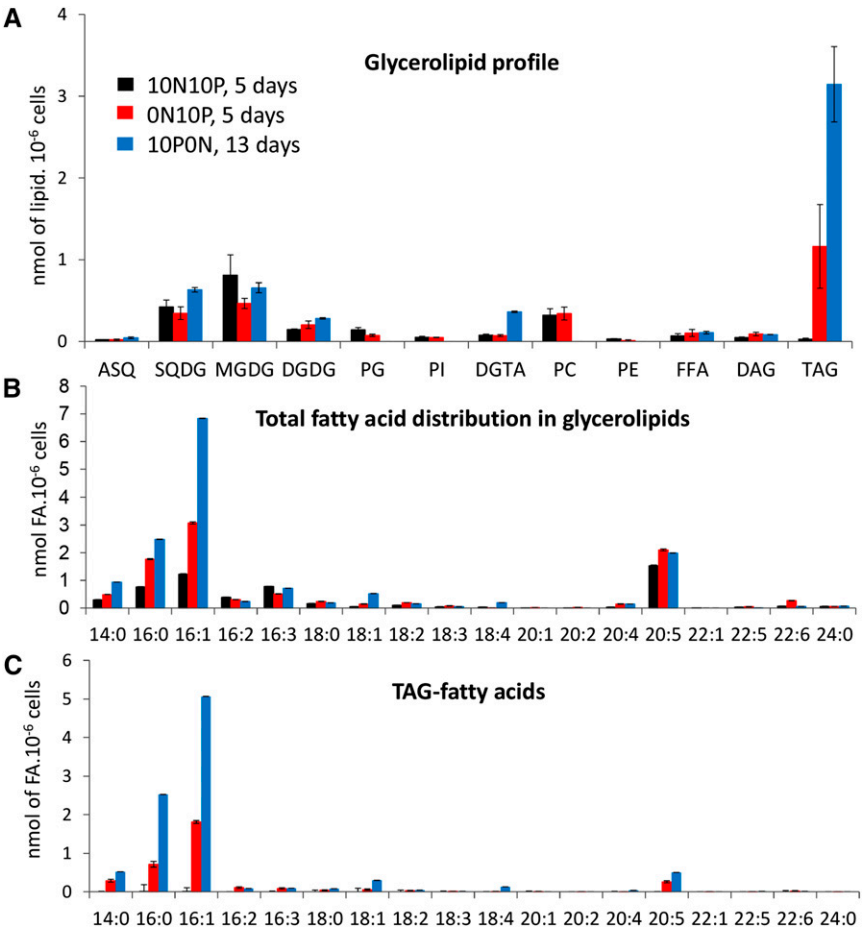

Figure 6. Quantitative analysis of FAs and glycerolipids in *P. tricornutum* grown in nutrient-replete conditions or in medium devoid of either N or P. Lipids from Pt1 cells grown either in a replete medium (10N10P; black) or in medium deprived of N (0N10P; blue) or P (10N0P; red) were extracted, separated by TLC, and quantified as described in "Materials and Methods." To avoid any N deficiency in 10N10P or 10N0P culture, media were replaced by fresh ESAW 10N10P or 10N0P medium every 3 d. Lipids were analyzed after 5 d of cultivation in replete conditions (black bars), N starvation (red bars), or after 13 d for P starvation (blue bars). A, Changes in glycerolipid content. Note that in the P-depleted condition, phospholipids were not detectable. B, Changes in FA content. C, FA profile in TAG. Each result is the average of three biological replicates ± SD. ASQ, Acyl-SQDG; FFA, free FAs.

Based on sequence similarity, we identified gene candidates for a plastid-localized synthesis of glycerolipids: a putative chloroplast glycerol-3-phosphate acyltransferase (ATS1 homolog; Phatr_3262), a chloroplast 1-acyl-*sn*-glycerol-3-phosphate acyltransferase (ATS2 homolog; Phat_43099), three MGDG synthase isoforms (three monogalactosyldiacyl homologs; Phatr_14125, Phatr_54168, and Phatr_9619), three DGDG synthase isoforms (three digalactosyldiacyl homologs; Phatr_12884, Phatr_11390, and Phatr_43116), a UDP-sulfoquinovose synthase (SQD1; Phatr_21201), and two SQDG synthase isoforms (two SQD2 homologs; Phatr_50356 and Phatr_42467). One or both of these SQD2 homologs also could be involved in the synthesis of ASQ.

The results obtained in this study indicate that FAs are synthesized in the stroma of chloroplasts by type II FA synthases, mainly as 14:0-, 16:0-, and 18:0-ACP. The presence of the saturated form of C18 in plastid lipids (i.e. 18:0) and the position of desaturation of $16:3^{\Delta 6,9,12}$ in MGDG (Domergue et al., 2003) suggest that the plastid Δ9-acyl-ACP desaturation might operate only on 16:0-ACP, releasing 16:1(ω-7)-ACP.

In plants, there are two pools of PG: one localized in the plastid, with a prokaryotic diacylglycerol backbone and a specific FA at the *sn*-2 position, 16:1(ω-13)t; and one in microsomal membranes and mitochondria, with a so-called eukaryotic diacylglycerol backbone assembled in the ER. In Arabidopsis, two enzymes are thus responsible for PG synthesis: Phosphatidylglycerophosphate synthase1 (PGP1), localized in both chloroplast and mitochondria (Babiychuk et al., 2003), and PGP2, localized in the ER (Müller and Frentzen, 2001). By studying *pgp* mutants, it was established that the PGP1-dependent pathway was responsible for 70% of PG synthesis in leaves and was required for the development of green leaves and chloroplasts with well-developed thylakoid membranes (Hagio et al., 2002; Xu et al., 2002), whereas the *pgp*2 mutant showed a small decrease in PG content compensated by a slight increase in PI content (Tanoue et al., 2014). Based on the facts that PG and PI biosynthesis pathways share their precursors (i.e. phosphatidic acid and cytidine diphosphate-diacylglycerol [CDP-DAG]) and that PGP2, the PI synthase, and the extraplastidic CDP-DAG synthases are all localized in the ER (Löfke et al., 2008; Zhou et al., 2013), the accumulation of PI in the Arabidopsis *pgp*2 mutant is consistent with an accumulation of CDP-DAG. In *P. tricornutum*, we found only two species of PG, the 20:5/16:1 form, which is probably plastidic with 16:1(ω-13)t at the *sn*-2 position, and the 16:1/16:0 form, which we expect to be extraplastidic, having exactly the same composition as PI. Together, these results suggest that the extraplastidic CDP-DAG synthase

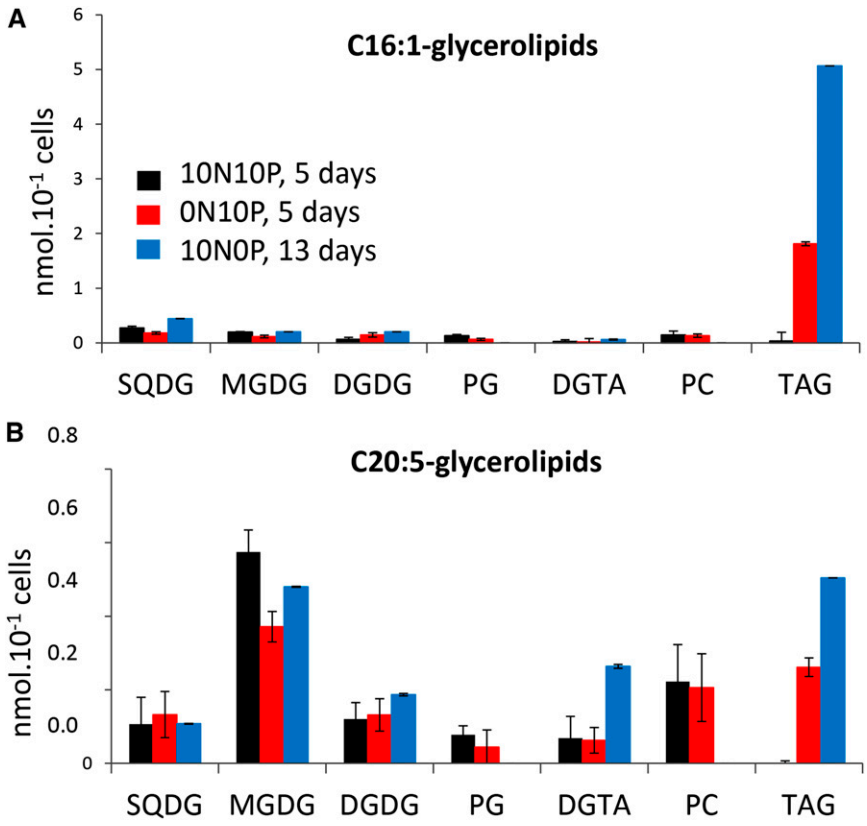

Figure 7. Distribution of 16:1 and 25:0 FAs in the glycerolipid classes of *P. tricornutum* grown in nutrient-replete conditions or in medium devoid of either N or P. Lipids from Pt1 cells grown in a replete medium (10N10P) were extracted, separated by TLC, and quantified as described in "Materials and Methods." Lipids were analyzed after 5 d of cultivation in replete condition (black bars), N starvation (red bars), or after 13 d of P starvation (blue bars). A, Quantitative distribution of 16:1 in the major glycerolipid classes. B, Quantitative distribution of 25:0 in the major glycerolipid classes. Each result is the average of three biological repeats ± SD.

is highly specific for a 16:1/16:0 substrate. Furthermore, the conservation of 16:0 at the *sn*-2 position in extraplastidic PG and PI in different algae species (Araki et al., 1987; Giroud et al., 1988; Liang et al., 2014) differs strikingly from the eukaryotic route observed in plants.

The preservation of the medium-chain FA in PI and extraplastidic PG might be important for their biological function. This result further supports either the absence of any FA selectivity of the extraplastidic LPAAT as being the basis of the plant eukaryotic signature or an export of the prokaryotic diacylglycerol backbone, as suggested in *C. reinhardtii* (Fan et al., 2011). In the *P. tricornutum* genome, two putative CDP-DAG synthases can be predicted (Phatr_559 and Phatr_7678), and future functional studies should help to ascertain whether one is specific for the production of PG/PI precursors.

In addition to the classical phospholipids that make up the bulk of nonphotosynthetic membranes, we report the presence of DGTA, a betaine glycerolipid never observed previously in *P. tricornutum*. BL have been detected in numerous algae (comprehensively reviewed by Dembitsky [1996]). Both DGTA and DGTS are usually associated with nonplastid membrane compartments (Künzler et al., 1997) and have structural similarities to PC (Sato and Murata, 1991). Therefore, we can speculate that DGTA might be more abundant in the endomembrane system and may be present in the outermost of the four membranes of the chloroplast, connected to the nuclear envelope. We identified a candidate gene that might be involved in BL synthesis, Phatr_42872, whose role should be assessed in the future based on functional genomics approaches.

Concerning FAs, eicopentaenoic acid (20:5) is the major molecular species, found in all membrane lipids of *P. tricornutum*. It is also a major FA in numerous microalgae, such as *Porphyridium cruentum* (Khozin et al., 1997), *N. gaditana* (Simionato et al., 2013), *Monodus subterraneus* (Khozin-Goldberg et al., 2002), and *Chromera velia* (Botté et al., 2011). This polyunsaturated very-long-chain FA is usually synthesized in the ER (Khozin et al., 1997) following complex desaturation and elongation processes (for review, see Petroutsos et al., 2014). The synthesis of 20:5 in the ER has not been unambiguously demonstrated in *P. tricornutum*. Nevertheless, the two front-end desaturases involved in this pathway, the Δ6 and Δ5 desaturases (Phatr_2948 and Phatr_46830, respectively), do not contain any predicted signal peptide and plastid-like transit sequence that could be involved in a targeting to the chloroplast. The synthesis of 20:5, therefore, is very likely to occur outside chloroplasts in *P. tricornutum* as well. The dominant species of MGDG in *M. subterraneus* (Khozin-Goldberg et al., 2002) and *P. cruentum* (Khozin et al., 1997) are 20:5/20:5. In these organisms, it was proposed that PE and PC were, respectively, donors for the DAG moiety responsible for these eukaryotic-like MGDG species. In *P. tricornutum*, however, all MGDG species having a 20:5 FA at the *sn*-1 position have a C16 at the *sn*-2 position, displaying a prokaryotic signature. Therefore, the acyl position in *P. tricornutum* MGDG supports a different

scenario from that documented for Arabidopsis eukaryotic MGDG: once synthesized in cytosolic membranes, 20:5 has to be released from a phospholipid into the cytosolic acyl-CoA pool and then transported into the chloroplasts to be attached to the glycerol-3-phosphate at the *sn*-1 position by the first acyltransferase, ATS1. We denoted this unique route, misleadingly thought to correspond to the plant eukaryotic pathway, the omega pathway (Petroutsos et al., 2014). The precise details and the enzymes and transporters involved in these events remain to be characterized.

The question of the putative existence of a eukaryotic pathway with a recycling of an intact diacylglycerol backbone coming from phospholipid for galactolipid synthesis, as described in higher plants, remains unsolved. Indeed, there is no visible signature for the eukaryotic pathway to follow, the typical eukaryotic 20:5/20:5 backbone found in extraplastidic glycerolipids (i.e. PC, PE, and DGTA) and described in other algae (Khozin et al., 1997; Khozin-Goldberg et al., 2002) being absent in plastid glycoglycerolipids. Since PC harbors a high proportion of C16 at the *sn*-2 position, we cannot exclude that some MGDG species could result from the galactosylation of a diacylglycerol backbone with this signature. However, considering that C18 is almost absent from galactoglycerolipids, this pathway should operate a sorting of diacyl molecular species, excluding PC with a C18 at position *sn*-2.

Remodeling of Membrane Glycerolipids in N- and P-Limiting Conditions

Based on our reference glycerolipid profile in a replete medium, we could compare the variations of the membrane lipid distribution occurring upon N or P starvation and attempt to deduce some likely remodeling scenarios. N shortage induces visible effects over a shorter time scale (3–4 d) compared with P shortage (8–13 d, depending on the initial level of this nutrient). This feature has been observed for all the Pt accessions examined here. Based on our observations, N limitation seems to trigger a serious and rapid stress response, presumably related to the need for protein synthesis, whereas more sophisticated lipid-remodeling systems seem to be operative during P limitation, perhaps as an adaptive response. This difference is also reflected at the level of photosynthesis; based on the F_v/F_m ratio, photosynthesis was apparently affected more rapidly in low-N than in low-P conditions.

Considering membrane glycerolipids, N deprivation has no effect on the level of N-containing lipids such as PC, PE, and DGTA. As in Arabidopsis, N-containing lipids are not a form of N storage (Gaude et al., 2007), in contrast with phospholipids, which are clearly a biochemical parameter tuned by photosynthetic organisms. The only significant changes we observed were a relative decrease of the proportion of MGDG and an increase in DGDG, leading to a diminished MGDG-DGDG ratio, a lipid change that also has been observed in Arabidopsis upon N shortage (Gaude et al., 2007). The physiological significance of this phenomenon is unknown, but a reduced MGDG-DGDG ratio is often observed in chloroplasts with impaired photosynthesis (Boudière et al., 2014). We could also detect a slight decrease in the proportion of PG, possibly reflecting senescence of the thylakoid membranes.

Following P deprivation, all phospholipids, including PC and PG, were completely undetectable, compensated by an increase of nonphosphorus lipids synthesized in endomembranes (indicated by a 5-fold-increase of DGTA) and in the plastid (indicated by a 2-fold increase of DGDG and a 1.5-fold increase of SQDG). The proportion of MGDG decreased by a factor of 1.5, but the overall proportion of galactoglycerolipids (MGDG and DGDG) increased. Similar observations have been made in higher plant cells (Jouhet et al., 2003), although the impact on phospholipids was not as dramatic as that recorded here. The best documented form of BL in the literature is DGTS, and, because it sometimes has an inverse concentration relationship with PC, it is thought to replace PC in extraplastidic membranes (Moore et al., 2001), as suggested for *C. reinhardtii*, which lacks PC (Riekhof et al., 2005, 2014), and further supported by the comparison of phytoplankton communities collected in P-rich and P-oligotrophic regions (Van Mooy et al., 2009). Consistent with this postulate, the increase of DGTA in the P-starved conditions reached a value that was about identical to that measured for PC in control cells, thus supporting that a PC-to-DGTA replacement occurred in extraplastidic membranes. In terms of lipid trafficking, no specific machinery would be required, since both DGTA and PC are likely synthesized in the same membrane system (i.e. the ER). It is also known that an increase of SQDG could compensate the absence of PG in plastids (Jouhet et al., 2010). Similarly, this remodeling would not require any massive lipid transport, since PG and SQDG are localized in the same membranes (i.e. thylakoids).

In plants, P deprivation induces an increase of galactolipid production, using a eukaryotic diacylglycerol moiety diverted from hydrolyzed phospholipids, and an export of DGDG from plastids to extraplastidic membranes, such as the plasma membrane, the tonoplast, and/or mitochondrial membranes (Andersson et al., 2003, 2005; Jouhet et al., 2004). First, based on our results, there is no evidence for a eukaryotic pathway in *P. tricornutum* as described in plants, but rather an omega pathway, which might participate in the recycling of the phospholipid hydrophobic moiety, possibly by free FA transfers. Second, in *P. tricornutum*, the plastid envelope contains four membranes, with the two outermost ones being derived from the ER. DGDG has never been found in the ER of higher plants, and this lipid is transferred toward mitochondria via contact sites, indicating that the ER is not involved in DGDG trafficking, at least for this interorganellar transfer (Jouhet et al., 2004). Similar physical links between the secondary plastid and the mitochondria might occur in *P. tricornutum*, since both organelles are very close (Prihoda et al., 2012). Third, the increase of

SQDG and DGTA could quantitatively compensate for the decrease of PG and PC, respectively. There is no obvious necessity for an export of DGDG toward extraplastidic membranes in the cells of *P. tricornutum* exposed to P limitation. It is possible, therefore, that an increase of DGDG, observed during both N and P limitation, might counteract the decrease of MGDG and contribute to the protection of photosynthetic membrane integrity.

In a recent report on the transcriptome changes occurring in *P. tricornutum* upon P shortage, transcripts for the ATS1 homolog (Phatr_3262), one of the MGDG synthase homologs (Phatr_54168), the two SQDG synthase isoforms (Phatr_50356 and Phatr_42467), and the putative gene involved in DGTA synthesis (Phatr_42872) were significantly up-regulated (Yang et al., 2014). Likewise, in the centric diatom *T. pseudonana*, genes coding two putative SQD1 homologs (gene identifiers 7445840 and 7452379) and two putative monogalactosyldiacyl homologs (gene identifiers 7447073 and 7445775) were found to be up-regulated in response to P limitation (Dyhrman et al., 2012). Therefore, the remodeling of lipids in diatoms seems to be transcriptionally controlled following, at least in part, the model dissected previously in plants, in which some of the genes encoding MGD, digalactosyldiacyl, and SQD2 isoforms (in Arabidopsis, MGD2, MGD3, DGD2, and SQD2; Misson et al., 2005) were shown to be specific to the P starvation response and activated by signaling cascades responding to low P. An in-depth study of the transcriptome of *P. tricornutum* cultivated in identical conditions to those used here will help identify all genes that are likely to be transcriptionally coordinated upstream of the observed remodeling and search for the corresponding cis-elements and transcriptional systems.

Accumulation of TAG in Conditions of N and P Starvation

All accessions of *P. tricornutum*, collected in various oceanic locations, showed an increase of TAG, albeit with some variations in the time scale and magnitude of accumulation of this class of nonpolar lipids. There was no apparent correlation between TAG accumulation and morphotype (triradiate, fusiform, or oval) or the initial geographic location. Pt10 and PtHK, which were both less sensitive to P shortage, were collected on the eastern coast of China, albeit at very distant sites, which could suggest an environmental impact on the physiology of these strains, perhaps with a higher capacity to store P. Interestingly, Pt4 was not able to accumulate large amounts of TAG in either N- or P-limiting conditions, which could suggest that it is affected in its ability to synthesize or store TAG. Pt4 was collected in the Baltic Sea, a relatively closed sea, but the long-term influence of this particular area on the physiological and metabolic behavior of these algae remains to be determined. Clearly, a genomic analysis of these strains is required to draw further conclusions.

P and N limitation affect both the lipid content and the photosynthetic capacities of Pt1 cells. Although N deprivation has a strong and almost immediate effect on cell division, it is important to note that P deprivation requires a much longer period to induce any visible effect. Diatoms, therefore, might struggle more with a lack of N than with a lack of P, possibly because of the existence of powerful P-storage systems within the cell, such as polyphosphate, a ubiquitous P polymer (Martin et al., 2014). N and P limitation will impact both the biosynthesis of proteins and the level of phosphorylated metabolites, which, in turn, will affect numerous metabolic functions, including growth and photosynthesis. However, oil accumulation depends on the availability of a carbon source (Fan et al., 2011), and this is in apparent contradiction with an increase of TAG concomitant with a decline of photosynthesis. In this study, this source of carbon possibly arises from the remaining photosynthetic activity and/or from stored carbohydrates (Li et al., 2011). Thus, it is likely that, in the case of a growth arrest linked to a mineral deficiency, the available carbon and energy unused for cell division and membrane expansion are diverted toward lipid biosynthesis and storage. This could be part of a cellular strategy to allow a better and quicker restart when environmental conditions become favorable again. Whether the arrest of cell division is an absolute requirement to trigger TAG accumulation is thus an important open question.

During both N and P shortages, we observed a significant increase in the neosynthesis of 16:0 and 16:1, which was mainly if not uniquely associated with the accumulation of TAG, whereas we observed only little change in the FA composition of the various glycerolipids, besides a 16:1 and 20:5 enrichment in TAG. This confirms previously published reports, in a variety of photosynthetic eukaryotes, showing that the accumulation of TAG triggered by a shortage of N originated mainly from FA neosynthesis (Simionato et al., 2013). Whatever the growth conditions, the small pool of DAG is constituted of three main species comprising only 14:0, 16:0, and 16:1 acyl groups, with 14:0 being less abundant than the others and always esterified at the *sn*-1 position, when present. Interestingly, the *sn*-1 and *sn*-2 positions in TAG completely mirror the DAG pool, and the *sn*-3 position is occupied by a 16:0 or 16:1 FA in 80% to 90% of the molecular species. These two FAs are also the main ones overproduced in nutrient-limiting growth conditions. Clearly, these data do not support any substantial recycling of DAG moieties deriving from membrane glycerolipids, by contrast with higher plants (Bates and Browse, 2012). Therefore, it is likely that TAGs are mostly synthesized via a route involving a diacylglycerol acyltransferase and de novo DAG and acyl-CoA synthesis (Kennedy pathway).

During both N and P limitation, TAGs were enriched in 20:5 at the *sn*-3 or *sn*-1 position, whereas the global level of 20:5 inside the cell was not affected. Since 20:5 is produced at the level of phospholipids in nonplastid membranes, it has to be transferred to TAG, most likely via the acyl-CoA pool or via a phosphatidyl diacylglycerol acyltransferase. In the N-deprived condition, it was striking to observe that the increase of 20:5 in TAG,

on a per cell basis, roughly corresponds to the decrease of 20:5 in MGDG, suggesting that MGDG also could contribute to TAG synthesis, as described in *N. graditana* (Simionato et al., 2013) and *C. reinhardtii* (Fan et al., 2011; Li et al., 2012). Based on this mechanism, the eicopentaenoic acid released in the acyl-CoA pool following the degradation of MGDG (or other membrane lipids such as phospholipids) should be recycled mainly into other glycerolipids such as TAG, rather than oxidized through the β-oxidation pathway.

CONCLUSION

The overall goal of this work was first to define a reference for the glycerolipidome of *P. tricornutum*, with MGDG, DGDG, SQDG, and PG as conserved lipids in photosynthetic membranes and PC and DGTA as major lipids in extraplastidic membranes. We also detected the presence of ASQ. Based on this reference, we could deduce that the FAs were most likely synthesized de novo in the stroma of chloroplasts as 14:0-, 16:0-, and 18:0-ACP species. We identified only one gene candidate coding for a putative palmitoyl-ACP Δ9-desaturase (Phatr_9316). When exported to the cytosol, FAs can be elongated and desaturated to generate 20:5. Acyl-ACP can be used in the plastid for the production of MGDG, DGDG, SQDG, and part of PG via a canonical prokaryotic pathway, and acyl-CoA can be used in the cytosol and endomembranes to generate PC, DGTA, or TAG. We could identify gene candidates coding for putative enzymes involved in these pathways. Extraplastidic PG and PI seem to share a common CDP-DAG precursor with a 16:1/16:0 signature. We could not detect any specific signature for an extraplastidic eukaryotic pathway as in plants and could not assess the possibility of the import of eukaryotic precursors inside the chloroplast. Rather, the plastid lipid profiles we obtained would be consistent with an import of 20:5 FAs, hydrolyzed from extraplastidic phospholipids, to serve as precursors for plastid acyltransferases, eventually producing MGDG, DGDG, and SQDG. We called this pathway the omega pathway, and future challenges include the deciphering of the machinery importing 20:5 FA into the chloroplast.

We compared the remodeling triggered by the deprivation of two major nutrients fluctuating in the oceans, N and P. On the one hand, N oligotrophy is apparently a severe stress for *P. tricornutum*, triggering a rapid senescence of chloroplast membranes, an arrest of cell division, and an accumulation of TAG. By contrast, a complex adaptation to P deprivation is observed, with a first phase of consumption of specific P-storage forms, most likely polyphosphate, followed by a breakdown of phospholipids, behaving like a secondary form of P storage, and their replacement by nonphosphorous lipids, most likely following PG-to-SQDG and PC-to-DGTA replacements. A phospholipid-to-DGDG replacement cannot be ruled out in some of the membranes limiting the chloroplast, but this has to be confirmed.

Future work should entail the characterization of the enzyme isoforms and the machineries for lipid synthesis, lipid breakdown, and lipid trafficking involved in the lipid changes described here and the systems controlling them. A survey of transcriptome variations occurring in *P. tricornutum* or *T. pseudonana* supports a transcriptional control, which should be studied further in the future. The task is as complex as that in plants, since some pathways, like the omega pathway, are apparently specific to chromalveolates, and their components cannot be deduced from previous studies. Nevertheless, the possibility to perform large-scale omics studies and to characterize the function of gene products is among the advantages of the *P. tricornutum* model. Future work starting with the gene candidates listed here will hopefully help to unravel the adaptive system of this diatom to cope with a fluctuating environment.

MATERIALS AND METHODS

Strains and Culture Conditions

Phaeodactylum tricornutum strains were obtained from the culture collections of the Pravosali-Guillard National Center for Culture of Marine Phytoplankton (CCMP) and the Culture Collection of Algae and Protozoa (CCAP), using axenic accessions characterized by De Martino et al. (2007): Pt1, CCAP 1055/3; Pt2, CCMP2558; Pt3, CCMP2559; Pt4, CCAP 1055/2; Pt5, CCMP630, Pt6 (fusiform), CCAP 1054/4; Pt7, CCAP 1055/6; Pt8, CCAP 1055/7; Pt9, CCAP 1055/5; Pt10, CCAP 1055/8. We completed this series of accessions with the fully sequenced reference strain for *P. tricornutum*, derived from Pt1, Pt1.8.6 (Bowler et al., 2008; CCAP1055/1), and with an axenic strain isolated in Hong Kong, PtHK. Cells were maintained and grown in enriched seawater, artificial water (ESAW) medium, as described by Falciatore et al. (2000). The different cell shapes described here are those of algae grown and maintained in artificial medium. In the preliminary comparative study of Pt1 to Pt10 ecotypes by microscopic imaging, cells were grown either in the presence of 0.55 mM N and 0.0224 mM P or in the absence of one or both of these nutrients. Cultures were grown in exponential phase in 50-mL single-use flasks with 100 rpm shaking, an irradiance of 100 μmol photons m^{-2} s^{-1}, and a 12-h-light/12-h-dark photoperiod at 19°C.

For the Nile Red measurements, 50-mL cultures were grown in exponential phase before being centrifuged at 1,500*g* for 30 min and suspended in 10 mL of replete or deficient medium. Initial cell densities for P-deficient and N-deficient experiments were 10^4 and 10^5 cells mL^{-1}, respectively. In the in-depth analysis performed on the Pt1 strain, cells were grown in batch conditions in 250-mL flasks containing 50 mL of ESAW medium with or without N or P. Replete conditions consisted of 5.5 mM N and 0.22 mM P, in order to avoid nutrient exhaustion in the batch culture over the observation period and to increase the contrast in the analyzed lipid profiles between nutrient-rich and -depleted conditions. Cells were cultivated in an artificial climate incubator, with 100 rpm shaking, under an irradiance of 40 μmol photons m^{-2} s^{-1} and with a 12-h-light/12-h-dark photoperiod at 19°C. The initial inoculum was 0.5 to 1.1^6 cells mL^{-1}. Cells were collected after 5 or 13 d and counted with a Malassez chamber using an aliquot fraction before any further manipulations.

Chlorophyll Fluorescence Measurements

The parameter F_v/F_m was used as an indicator of PSII activity in a dark-adapted state. For this, in vivo chlorophyll fluorescence was determined using a Speedzen MX fluorescence imaging setup (JBeamBio). Excitation was done in the blue range (λ = 450 nm) using short pulses (10 μs). Emission was measured in the near far red. Saturating pulses (duration of 250 ms) were provided by a green (λ = 520 nm) light-emitting diode array. Measurements were done 15 min after dark adaptation of the samples.

The variable fluorescence (F_v) was calculated as $F_v = F_m - F_o$, where F_m is the maximum fluorescence in the dark-adapted state and F_o is the minimal fluorescence in the dark-adapted state (Genty et al., 1990).

Nile Red Staining of Nonpolar Lipids

Accumulation of nonpolar lipids and oil droplets was monitored by Nile Red (Sigma-Aldrich) fluorescent staining (excitation wavelength at 532 nm and emission at 565 nm), as described previously (Cooksey et al., 1987). In brief, 200 μL of culture was stained with 50 μL of a Nile Red stock solution (2.5 μg mL^{-1} in dimethyl sulfoxide), and fluorescence was measured by flow cytometry using a Partec Cube8 device equipped with a 532-nm green laser. When the number of cells was estimated, specific fluorescence was determined by dividing Nile Red fluorescence intensity by the number of cells.

Glycerolipid Extraction, Separation by TLC, and Analyses by GC-FID and MS

Glycerolipids were extracted from freeze-dried *P. tricornutum* cells grown in 50 mL of ESAW medium with variable initial supplies of P and/or N. First, cells were harvested by centrifugation and then immediately frozen in liquid N. Once freeze dried, the pellet was suspended in 4 mL of boiling ethanol for 5 min to prevent lipid degradation, and lipids were extracted according to Simionato et al. (2013) by the addition of 2 mL of methanol and 8 mL of chloroform at room temperature. The mixture was then saturated with argon and stirred for 1 h at room temperature. After filtration through glass wool, cell debris was rinsed with 3 mL of chloroform:methanol (2:1, v/v), and 5 mL of 1% (w/v) NaCl was then added to the filtrate to initiate biphase formation. The chloroform phase was dried under argon before solubilizing the lipid extract in pure chloroform.

Total glycerolipids were quantified from their FAs: in an aliquot fraction, a known quantity of 15:0 was added and the FAs present were transformed as FAMEs by a 1-h incubation in 3 mL of 2.5% (v/v) H_2SO_4 in pure methanol at 100°C (Jouhet et al., 2003). The reaction was stopped by the addition of 3 mL of water and 3 mL of hexane. The hexane phase was analyzed by a GC-FID (Perkin-Elmer) on a BPX70 (SGE) column. FAMEs were identified by comparison of their retention times with those of standards (Sigma-Aldrich) and quantified by the surface peak method using 15:0 for calibration. Extraction and quantification were performed at least three times.

To quantify the various classes of nonpolar and polar glycerolipids, lipids were separated by TLC onto glass-backed silica gel plates (Merck) using two distinct resolving systems (Simionato et al., 2013). To isolate nonpolar lipids including TAG and free FA, lipids were resolved by TLC run in one dimension with hexane:diethylether:acetic acid (70:30:1, v/v). To isolate membrane glycerolipids, lipids were resolved by two-dimensional TLC. The first solvent was chloroform:methanol:water (65:25:4, v/v) and the second was chloroform:acetone:methanol:acetic acid:water (50:20:10:10:5, v/v). Lipids were then visualized under UV light, after spraying with 2% (v/v) 8-anilino-1-naphthalenesulfonic acid in methanol, and scraped off the plate. No phosphatidylethanol could be detected after TLC or following MS analyses, indicating that the boiling ethanol treatment did not give rise to this category of glycerolipid derivative by nonspecific chemical reactions. Lipids were recovered from the silica powder after the addition of 1.35 mL of chloroform:methanol (1:2, v/v) thorough mixing, the addition of 0.45 mL of chloroform and 0.8 mL of water, and collection of the chloroform phase (Bligh and Dyer, 1959). Lipids were then dried under argon and either quantified by methanolysis and GC-FID as described above or analyzed by MS.

For MS analyses, purified lipid classes were dissolved in 10 mM ammonium acetate in pure methanol. They were introduced by direct infusion (electrospray ionization-MS) into a trap-type mass spectrometer (LTQ-XL; Thermo Scientific) and identified by comparison with standards. In these conditions, the produced ions were mainly present as H^-, H^+, NH_4^+, or Na^+ adducts. Lipids were identified by MS2 analysis with their precursor ion or by neutral loss analyses as indicated in Table I. All experiments were performed in triplicate.

Positional Distribution of FAs Esterified to Glycerolipids

The positions of FA molecular species esterified to the glycerol backbone of the various glycerolipids were determined based on MS2 analyses. Glycerol carbons were numbered following the stereospecific number (*sn*) nomenclature. Depending on the nature of the glycerolipid and the type of adduct, the substituents at the *sn*-1 (or *sn*-3) and *sn*-2 positions are differently cleaved when subjected to low-energy collision-induced dissociation. This is reflected in MS2 analyses by the preferential loss of one of the two FAs, leading to a dissymmetrical abundance of the collision fragments. The patterns of MS2 fragments for all glycerolipids have been described in previous studies (Table II), except for DGTA. In this study, we hypothesized that the loss of FAs in DGTA following low-energy collision-induced dissociation is similar to that observed for other polar lipids, such as PC.

Supplemental Data

The following supplemental materials are available.

Supplemental Figure S1. Growth, photosynthetic activity, and intracellular triacylglycerol content of Pt1 cells in 1N1P and 10N10P conditions.

Supplemental Figure S2. Growth, photosynthetic activity, and intracellular triacylglycerol content of Pt1 cells in 10N10P, 0N10P, and 10N0P conditions.

Supplemental Figure S3. General structure of glycerolipids.

Supplemental Figure S4. Structural analysis of ASQ.

ACKNOWLEDGMENTS

We thank Yahui Gao (Xiamen University), who kindly provided the PtHK strain isolated in Hong Kong Harbor in October 2010, and Catherine Cantrel (Institut de Biologie de l'École Normale Supérieure), Mathilde Cussac, Valérie Gros, and Guillaume Tourcier (Laboratoire de Physiologie Cellulaire et Végétale) for helpful technical support.

Received October 23, 2014; accepted December 5, 2014; published December 8, 2014.

LITERATURE CITED

Allen AE, Laroche J, Maheswari U, Lommer M, Schauer N, Lopez PJ, Finazzi G, Fernie AR, Bowler C (2008) Whole-cell response of the pennate diatom Phaeodactylum tricornutum to iron starvation. Proc Natl Acad Sci USA **105:** 10438–10443

Alonso DL, Belarbi EH, Fernández-Sevilla JM, Rodríguez-Ruiz J, Molina Grima E (2000) Acyl lipid composition variation related to culture age and nitrogen concentration in continuous culture of the microalga Phaeodactylum tricornutum. Phytochemistry **54:** 461–471

Andersson MX, Larsson KE, Tjellström H, Liljenberg C, Sandelius AS (2005) Phosphate-limited oat: the plasma membrane and the tonoplast as major targets for phospholipid-to-glycolipid replacement and stimulation of phospholipases in the plasma membrane. J Biol Chem **280:** 27578–27586

Andersson MX, Stridh MH, Larsson KE, Liljenberg C, Sandelius AS (2003) Phosphate-deficient oat replaces a major portion of the plasma membrane phospholipids with the galactolipid digalactosyldiacylglycerol. FEBS Lett **537:** 128–132

Araki S, Sakurai T, Kawaguchi A, Murata N (1987) Positional distribution of fatty acids in glycerolipids of the marine red alga, Porphyra yezoensis. Plant Cell Physiol **28:** 761–766

Arao T, Kawaguchi A, Yamada M (1987) Positional distribution of fatty acids in lipids of the marine diatom Phaeodactylum tricornutum. Phytochemistry **26:** 2573–2576

Armada I, Hachero-Cruzado I, Mazuelos N, Ríos JL, Manchado M, Cañavate JP (2013) Differences in betaine lipids and fatty acids between Pseudoisochrysis paradoxa VLP and Diacronema vlkianum VLP isolates (Haptophyta). Phytochemistry **95:** 224–233

Armbrust EV, Berges JA, Bowler C, Green BR, Martinez D, Putnam NH, Zhou S, Allen AE, Apt KE, Bechner M, et al (2004) The genome of the diatom Thalassiosira pseudonana: ecology, evolution, and metabolism. Science **306:** 79–86

Babiychuk E, Müller F, Eubel H, Braun HP, Frentzen M, Kushnir S (2003) Arabidopsis phosphatidylglycerophosphate synthase 1 is essential for chloroplast differentiation, but is dispensable for mitochondrial function. Plant J **33:** 899–909

Bates PD, Browse J (2012) The significance of different diacylgycerol synthesis pathways on plant oil composition and bioengineering. Front Plant Sci **3:** 147

Benning C, Ohta H (2005) Three enzyme systems for galactoglycerolipid biosynthesis are coordinately regulated in plants. J Biol Chem **280:** 2397–2400

Bligh EG, Dyer WJ (1959) A rapid method of total lipid extraction and purification. Can J Biochem Physiol **37:** 911–917

Botté CY, Yamaryo-Botté Y, Janouskovec J, Rupasinghe T, Keeling PJ, Crellin P, Coppel RL, Maréchal E, McConville MJ, McFadden GI (2011) Identification of plant-like galactolipids in Chromera velia, a photosynthetic relative of malaria parasites. J Biol Chem **286:** 29893–29903

Boudière L, Botté CY, Saidani N, Lajoie M, Marion J, Bréhélin L, Yamaryo-Botté Y, Satiat-Jeunemaître B, Breton C, Girard-Egrot A, et al (2012) Galvestine-1, a novel chemical probe for the study of the glycerolipid homeostasis system in plant cells. Mol Biosyst **8:** 2023–2035

Boudière L, Michaud M, Petroutsos D, Rébeillé F, Falconet D, Bastien O, Roy S, Finazzi G, Rolland N, Jouhet J, et al (2014) Glycerolipids in photosynthesis: composition, synthesis and trafficking. Biochim Biophys Acta **1837:** 470–480

Bowler C, Allen AE, Badger JH, Grimwood J, Jabbari K, Kuo A, Maheswari U, Martens C, Maumus F, Otillar RP, et al (2008) The Phaeodactylum genome reveals the evolutionary history of diatom genomes. Nature **456:** 239–244

Brighouse A, Dacks JB, Field MC (2010) Rab protein evolution and the history of the eukaryotic endomembrane system. Cell Mol Life Sci **67:** 3449–3465

Browse J, Warwick N, Somerville CR, Slack CR (1986) Fluxes through the prokaryotic and eukaryotic pathways of lipid synthesis in the '16:3' plant Arabidopsis thaliana. Biochem J **235:** 25–31

Brügger B, Erben G, Sandhoff R, Wieland FT, Lehmann WD (1997) Quantitative analysis of biological membrane lipids at the low picomole level by nano-electrospray ionization tandem mass spectrometry. Proc Natl Acad Sci USA **94:** 2339–2344

Camera E, Ludovici M, Galante M, Sinagra JL, Picardo M (2010) Comprehensive analysis of the major lipid classes in sebum by rapid resolution high-performance liquid chromatography and electrospray mass spectrometry. J Lipid Res **51:** 3377–3388

Chauton MS, Winge P, Brembu T, Vadstein O, Bones AM (2013) Gene regulation of carbon fixation, storage, and utilization in the diatom *Phaeodactylum tricornutum* acclimated to light/dark cycles. Plant Physiol **161:** 1034–1048

Cooksey KE, Guckert B, Williams SA, Callis PR (1987) Fluorometric determination of the neutral lipid content of microalgal cells using Nile Red. J Microbiol Methods **6:** 333–345

Davidi L, Shimoni E, Khozin-Goldberg I, Zamir A, Pick U (2014) Origin of β-carotene-rich plastoglobuli in *Dunaliella bardawil*. Plant Physiol **164:** 2139–2156

De Martino A, Meichenin A, Shi J, Pan K, Bowler C (2007) Genetic and phenotypic characterization of Phaeodactylum tricornutum (Bacillariophyceae) accessions. J Phycol **43:** 992–1009

Dembitsky VM (1996) Betaine ether-linked glycerolipids: chemistry and biology. Prog Lipid Res **35:** 1–51

Dodson VJ, Mouget JL, Dahmen JL, Leblond JD (2014) The long and short of it: temperature-dependent modifications of fatty acid chain length and unsaturation in the galactolipid profiles of the diatoms Haslea ostrearia and Phaeodactylum tricornutum. Hydrobiologia **727:** 95–107

Domergue F, Spiekermann P, Lerchl J, Beckmann C, Kilian O, Kroth PG, Boland W, Zähringer U, Heinz E (2003) New insight into *Phaeodactylum tricornutum* fatty acid metabolism: cloning and functional characterization of plastidial and microsomal Δ12-fatty acid desaturases. Plant Physiol **131:** 1648–1660

Domingues P, Amado FML, Santana-Marques MGO, Ferrer-Correia AJ (1998) Constant neutral loss scanning for the characterization of glycerol phosphatidylcholine phospholipids. J Am Soc Mass Spectrom **9:** 1189–1195

Dorrell RG, Smith AG (2011) Do red and green make brown? Perspectives on plastid acquisitions within chromalveolates. Eukaryot Cell **10:** 856–868

Dubots E, Audry M, Yamaryo Y, Bastien O, Ohta H, Breton C, Maréchal E, Block MA (2010) Activation of the chloroplast monogalactosyldiacylglycerol synthase MGD1 by phosphatidic acid and phosphatidylglycerol. J Biol Chem **285:** 6003–6011

Dubots E, Botté C, Boudière L, Yamaryo-Botté Y, Jouhet J, Maréchal E, Block MA (2012) Role of phosphatidic acid in plant galactolipid synthesis. Biochimie **94:** 86–93

Dyhrman ST, Jenkins BD, Rynearson TA, Saito MA, Mercier ML, Alexander H, Whitney LP, Drzewianowski A, Bulygin VV, Bertrand EM, et al (2012) The transcriptome and proteome of the diatom Thalassiosira pseudonana reveal a diverse phosphorus stress response. PLoS ONE **7:** e33768

Falciatore A, d'Alcalà MR, Croot P, Bowler C (2000) Perception of environmental signals by a marine diatom. Science **288:** 2363–2366

Fan J, Andre C, Xu C (2011) A chloroplast pathway for the de novo biosynthesis of triacylglycerol in Chlamydomonas reinhardtii. FEBS Lett **585:** 1985–1991

Frentzen M, Heinz E, McKeon TA, Stumpf PK (1983) Specificities and selectivities of glycerol-3-phosphate acyltransferase and monoacylglycerol-3-phosphate acyltransferase from pea and spinach chloroplasts. Eur J Biochem **129:** 629–636

Gage DA, Huang ZH, Benning C (1992) Comparison of sulfoquinovosyl diacylglycerol from spinach and the purple bacterium Rhodobacter spaeroides by fast atom bombardment tandem mass spectrometry. Lipids **27:** 632–636

Gaude N, Bréhélin C, Tischendorf G, Kessler F, Dörmann P (2007) Nitrogen deficiency in Arabidopsis affects galactolipid composition and gene expression and results in accumulation of fatty acid phytyl esters. Plant J **49:** 729–739

Genty B, Harbinson J, Briantais JM, Baker NR (1990) The relationship between non-photochemical quenching of chlorophyll fluorescence and the rate of photosystem 2 photochemistry in leaves. Photosynth Res **25:** 249–257

Giroud C, Gerber A, Eichenberger W (1988) Lipids of Chlamydomonas reinhardtii: analysis of molecular species and intracellular site(s) of biosynthesis. Plant Cell Physiol **29:** 587–595

Guella G, Frassanito R, Mancini I (2003) A new solution for an old problem: the regiochemical distribution of the acyl chains in galactolipids can be established by electrospray ionization tandem mass spectrometry. Rapid Commun Mass Spectrom **17:** 1982–1994

Guschina IA, Harwood JL (2006) Lipids and lipid metabolism in eukaryotic algae. Prog Lipid Res **45:** 160–186

Hagio M, Sakurai I, Sato S, Kato T, Tabata S, Wada H (2002) Phosphatidylglycerol is essential for the development of thylakoid membranes in Arabidopsis thaliana. Plant Cell Physiol **43:** 1456–1464

Hecky RE, Kilham P (1988) Nutrient limitation of phytoplankton in freshwater and marine environments. Limnol Oceanogr **33:** 786–822

Hsu FF, Turk J (2000a) Characterization of phosphatidylethanolamine as a lithiated adduct by triple quadrupole tandem mass spectrometry with electrospray ionization. J Mass Spectrom **35:** 595–606

Hsu FF, Turk J (2000b) Characterization of phosphatidylinositol, phosphatidylinositol-4-phosphate, and phosphatidylinositol-4,5-bisphosphate by electrospray ionization tandem mass spectrometry: a mechanistic study. J Am Soc Mass Spectrom **11:** 986–999

Hsu FF, Turk J (2001) Studies on phosphatidylglycerol with triple quadrupole tandem mass spectrometry with electrospray ionization: fragmentation processes and structural characterization. J Am Soc Mass Spectrom **12:** 1036–1043

Hsu FF, Turk J (2003) Electrospray ionization/tandem quadrupole mass spectrometric studies on phosphatidylcholines: the fragmentation processes. J Am Soc Mass Spectrom **14:** 352–363

Hsu FF, Turk J (2010) Electrospray ionization multiple-stage linear ion-trap mass spectrometry for structural elucidation of triacylglycerols: assignment of fatty acyl groups on the glycerol backbone and location of double bonds. J Am Soc Mass Spectrom **21:** 657–669

Jouhet J, Dubots E, Maréchal E, Block MA (2010) Lipid trafficking in plant photosynthetic cells. *In* **H Wada, N Murata**, eds, Lipids in Photosynthesis, **Vol 30**. Springer, Dordrecht, The Netherlands, pp 349–372

Jouhet J, Maréchal E, Baldan B, Bligny R, Joyard J, Block MA (2004) Phosphate deprivation induces transfer of DGDG galactolipid from chloroplast to mitochondria. J Cell Biol **167:** 863–874

Jouhet J, Maréchal E, Bligny R, Joyard J, Block MA (2003) Transient increase of phosphatidylcholine in plant cells in response to phosphate deprivation. FEBS Lett **544:** 63–68

Jouhet J, Maréchal E, Block MA (2007) Glycerolipid transfer for the building of membranes in plant cells. Prog Lipid Res **46:** 37–55

Khozin I, Adlerstein D, Bigongo C, Heimer YM, Cohen Z (1997) Elucidation of the biosynthesis of eicosapentaenoic acid in the microalga *Porphyridium cruentum*: II. Studies with radiolabeled precursors. Plant Physiol **114:** 223–230

Khozin-Goldberg I, Didi-Cohen S, Shayakhmetova I, Cohen Z (2002) Biosynthesis of eicopentaenoic acid (EPA) in the fresh water eustigmatophyte Monodus subterraneaus (Eustigmatophyceae). J Phycol **38:** 745–756

Kroth PG, Chiovitti A, Gruber A, Martin-Jezequel V, Mock T, Parker MS, Stanley MS, Kaplan A, Caron L, Weber T, et al (2008) A model for

carbohydrate metabolism in the diatom Phaeodactylum tricornutum deduced from comparative whole genome analysis. PLoS ONE **3:** e1426

Künzler K, Eichenberger W, Radunz A (1997) Intracellular localization of two betaine lipids by cell fractionation and immunomicroscopy. Z Naturforsch C **52:** 487–495

Levitan O, Dinamarca J, Hochman G, Falkowski PG (2014) Diatoms: a fossil fuel of the future. Trends Biotechnol **32:** 117–124

Li X, Moellering ER, Liu B, Johnny C, Fedewa M, Sears BB, Kuo MH, Benning C (2012) A galactoglycerolipid lipase is required for triacylglycerol accumulation and survival following nitrogen deprivation in *Chlamydomonas reinhardtii*. Plant Cell **24:** 4670–4686

Li Y, Han D, Sommerfeld M, Hu Q (2011) Photosynthetic carbon partitioning and lipid production in the oleaginous microalga Pseudochlorococcum sp. (Chlorophyceae) under nitrogen-limited conditions. Bioresour Technol **102:** 123–129

Liang Y, Maeda Y, Yoshino T, Matsumoto M, Tanaka T (2014) Profiling of polar lipids in marine oleaginous diatom Fistulifera solaris JPCC DA0580: prediction of the potential mechanism for eicosapentaenoic acid-incorporation into triacylglycerol. Mar Drugs **12:** 3218–3230

Li-Beisson Y, Shorrosh B, Beisson F, Andersson MX, Arondel V, Bates PD, Baud S, Bird D, Debono A, Durrett TP, et al (2010) Acyl-lipid metabolism. The Arabidopsis Book **8:** e0133, doi/10.1199/tab.0161

Litchman E, Klausmeier CA, Yoshiyama K (2009) Contrasting size evolution in marine and freshwater diatoms. Proc Natl Acad Sci USA **106:** 2665–2670

Löfke C, Ischebeck T, König S, Freitag S, Heilmann I (2008) Alternative metabolic fates of phosphatidylinositol produced by phosphatidylinositol synthase isoforms in Arabidopsis thaliana. Biochem J **413:** 115–124

Maheswari U, Mock T, Armbrust EV, Bowler C (2009) Update of the Diatom EST Database: a new tool for digital transcriptomics. Nucleic Acids Res **37:** D1001–D1005

Maheswari U, Montsant A, Goll J, Krishnasamy S, Rajyashri KR, Patell VM, Bowler C (2005) The Diatom EST Database. Nucleic Acids Res **33:** D344–D347

Maréchal E, Block MA, Joyard J, Douce R (1994) Kinetic properties of monogalactosyldiacylglycerol synthase from spinach chloroplast envelope membranes. J Biol Chem **269:** 5788–5798

Martin P, Dyhrman ST, Lomas MW, Poulton NJ, Van Mooy BAS (2014) Accumulation and enhanced cycling of polyphosphate by Sargasso Sea plankton in response to low phosphorus. Proc Natl Acad Sci USA **111:** 8089–8094

Mills MM, Ridame C, Davey M, La Roche J, Geider RJ (2004) Iron and phosphorus co-limit nitrogen fixation in the eastern tropical North Atlantic. Nature **429:** 292–294

Misson J, Raghothama KG, Jain A, Jouhet J, Block MA, Bligny R, Ortet P, Creff A, Somerville S, Rolland N, et al (2005) A genome-wide transcriptional analysis using Arabidopsis thaliana Affymetrix gene chips determined plant responses to phosphate deprivation. Proc Natl Acad Sci USA **102:** 11934–11939

Mongrand S, Bessoule JJ, Cabantous F, Cassagne C (1998) The C16:3/C18:3 fatty acid balance in photosynthetic tissues from 468 plant species. Phytochemistry **49:** 1049–1064

Montsant A, Maheswari U, Bowler C, Lopez PJ (2005) Diatomics: toward diatom functional genomics. J Nanosci Nanotechnol **5:** 5–14

Moore C, Mills M, Arrigo K, Berman-Frank I, Bopp L, Boyd P, Galbraith E, Geider R, Guieu C, Jaccard S, et al (2013) Processes and patterns of oceanic nutrient limitation. Nat Geosci **6:** 701–710

Moore TS, Du Z, Chen Z (2001) Membrane lipid biosynthesis in *Chlamydomonas reinhardtii*: in vitro biosynthesis of diacylglyceryltrimethylhomoserine. Plant Physiol **125:** 423–429

Morcuende R, Bari R, Gibon Y, Zheng W, Pant BD, Bläsing O, Usadel B, Czechowski T, Udvardi MK, Stitt M, et al (2007) Genome-wide reprogramming of metabolism and regulatory networks of Arabidopsis in response to phosphorus. Plant Cell Environ **30:** 85–112

Moreau RA, Doehlert DC, Welti R, Isaac G, Roth M, Tamura P, Nuñez A (2008) The identification of mono-, di-, tri-, and tetragalactosyl-diacylglycerols and their natural estolides in oat kernels. Lipids **43:** 533–548

Müller F, Frentzen M (2001) Phosphatidylglycerophosphate synthases from Arabidopsis thaliana. FEBS Lett **509:** 298–302

Nakamura Y (2013) Phosphate starvation and membrane lipid remodeling in seed plants. Prog Lipid Res **52:** 43–50

Naumann I, Klein BC, Bartel SJ, Darsow KH, Buchholz R, Lange HA (2011) Identification of sulfoquinovosyldiacylglycerides from Phaeodactylum tricornutum by matrix-assisted laser desorption/ionization QTrap time-of-flight hybrid mass spectrometry. Rapid Commun Mass Spectrom **25:** 2517–2523

Nunn BL, Aker JR, Shaffer SA, Tsai S, Strzepek RF, Boyd PW, Freeman TL, Brittnacher M, Malmström L, Goodlett DR (2009) Deciphering diatom biochemical pathways via whole-cell proteomics. Aquat Microb Ecol **55:** 241–253

Petroutsos D, Amiar S, Abida H, Dolch LJ, Bastien O, Rébeillé F, Jouhet J, Falconet D, Block MA, McFadden GI, et al (2014) Evolution of galactoglycerolipid biosynthetic pathways: from cyanobacteria to primary plastids and from primary to secondary plastids. Prog Lipid Res **54:** 68–85

Prihoda J, Tanaka A, de Paula WBM, Allen JF, Tirichine L, Bowler C (2012) Chloroplast-mitochondria cross-talk in diatoms. J Exp Bot **63:** 1543–1557

Rezanka T, Lukavský J, Nedbalová L, Sigler K (2011) Effect of nitrogen and phosphorus starvation on the polyunsaturated triacylglycerol composition, including positional isomer distribution, in the alga Trachydiscus minutus. Phytochemistry **72:** 2342–2351

Riekhof WR, Naik S, Bertrand H, Benning C, Voelker DR (2014) Phosphate starvation in fungi induces the replacement of phosphatidylcholine with the phosphorus-free betaine lipid diacylglyceryl-N,N,N-trimethylhomoserine. Eukaryot Cell **13:** 749–757

Riekhof WR, Ruckle ME, Lydic TA, Sears BB, Benning C (2003) The sulfolipids 2′-*O*-acyl-sulfoquinovosyldiacylglycerol and sulfoquinovosyldiacylglycerol are absent from a *Chlamydomonas reinhardtii* mutant deleted in *SQD1*. Plant Physiol **133:** 864–874

Riekhof WR, Sears BB, Benning C (2005) Annotation of genes involved in glycerolipid biosynthesis in Chlamydomonas reinhardtii: discovery of the betaine lipid synthase BTA1Cr. Eukaryot Cell **4:** 242–252

Sandelius AS, Andersson MX, Goksor M, Tjellstrom H, Wellander R (2007) Membrane contact sites: physical attachment between chloroplasts and endoplasmic reticulum revealed by optical manipulation. Chem Phys Lipids **149:** S42–S43

Sapriel G, Quinet M, Heijde M, Jourdren L, Tanty V, Luo G, Le Crom S, Lopez PJ (2009) Genome-wide transcriptome analyses of silicon metabolism in Phaeodactylum tricornutum reveal the multilevel regulation of silicic acid transporters. PLoS ONE **4:** e7458

Sato N, Murata N (1991) Transition of lipid phase in aqueous dispersions of diacylglyceryltrimethylhomoserine. Biochim Biophys Acta **1082:** 108–111

Scala S, Bowler C (2001) Molecular insights into the novel aspects of diatom biology. Cell Mol Life Sci **58:** 1666–1673

Shimojima M, Ohta H (2011) Critical regulation of galactolipid synthesis controls membrane differentiation and remodeling in distinct plant organs and following environmental changes. Prog Lipid Res **50:** 258–266

Shrestha RP, Tesson B, Norden-Krichmar T, Federowicz S, Hildebrand M, Allen AE (2012) Whole transcriptome analysis of the silicon response of the diatom Thalassiosira pseudonana. BMC Genomics **13:** 499

Simionato D, Block MA, La Rocca N, Jouhet J, Maréchal E, Finazzi G, Morosinotto T (2013) The response of Nannochloropsis gaditana to nitrogen starvation includes de novo biosynthesis of triacylglycerols, a decrease of chloroplast galactolipids, and reorganization of the photosynthetic apparatus. Eukaryot Cell **12:** 665–676

Taguchi R, Houjou T, Nakanishi H, Yamazaki T, Ishida M, Imagawa M, Shimizu T (2005) Focused lipidomics by tandem mass spectrometry. J Chromatogr B Analyt Technol Biomed Life Sci **823:** 26–36

Tanoue R, Kobayashi M, Katayama K, Nagata N, Wada H (2014) Phosphatidylglycerol biosynthesis is required for the development of embryos and normal membrane structures of chloroplasts and mitochondria in Arabidopsis. FEBS Lett **588:** 1680–1685

Tjellström H, Andersson MX, Larsson KE, Sandelius AS (2008) Membrane phospholipids as a phosphate reserve: the dynamic nature of phospholipid-to-digalactosyl diacylglycerol exchange in higher plants. Plant Cell Environ **31:** 1388–1398

Van Mooy BAS, Fredricks HF, Pedler BE, Dyhrman ST, Karl DM, Koblízek M, Lomas MW, Mincer TJ, Moore LR, Moutin T, et al (2009) Phytoplankton in the ocean use non-phosphorus lipids in response to phosphorus scarcity. Nature **458:** 69–72

Vogel G, Eichenberger W (1992) Betaine lipids in lower plants: biosynthesis of DGTS and DGTA in Ochromonas danica (Chrysophyceae) and the possible role of DGTS in lipid metabolism. Plant Cell Physiol **33:** 427–436

Welti R, Wang X, Williams TD (2003) Electrospray ionization tandem mass spectrometry scan modes for plant chloroplast lipids. Anal Biochem **314:** 149–152

Xu C, Härtel H, Wada H, Hagio M, Yu B, Eakin C, Benning C (2002) The *pgp1* mutant locus of Arabidopsis encodes a phosphatidylglycerolphosphate synthase with impaired activity. Plant Physiol **129:** 594–604

Yang ZK, Zheng JW, Niu YF, Yang WD, Liu JS, Li HY (2014) Systems-level analysis of the metabolic responses of the diatom Phaeodactylum tricornutum to phosphorus stress. Environ Microbiol **16:** 1793–1807

Yongmanitchai W, Ward OP (1993) Positional distribution of fatty acids, and molecular species of polar lipids, in the diatom Phaeodactylum tricornutum. J Gen Microbiol **139:** 465–472

Zendejas FJ, Benke PI, Lane PD, Simmons BA, Lane TW (2012) Characterization of the acylglycerols and resulting biodiesel derived from vegetable oil and microalgae (Thalassiosira pseudonana and Phaeodactylum tricornutum). Biotechnol Bioeng **109:** 1146–1154

Zhou Y, Peisker H, Weth A, Baumgartner W, Dörmann P, Frentzen M (2013) Extraplastidial cytidinediphosphate diacylglycerol synthase activity is required for vegetative development in Arabidopsis thaliana. Plant J **75:** 867–879

Zianni R, Bianco G, Lelario F, Losito I, Palmisano F, Cataldi TR (2013) Fatty acid neutral losses observed in tandem mass spectrometry with collision-induced dissociation allows regiochemical assignment of sulfoquinovosyldiacylglycerols. J Mass Spectrom **48:** 205–215